Virtual Screening Directly Identifies New Fragment-Sized Inhibitors of Carboxylesterase Notum with Nanomolar Activity

David Steadman,[1] Benjamin N. Atkinson,[1] Yuguang Zhao,[2] Nicky J. Willis,[1] Sarah Frew,[1] Amy Monaghan,[1] Chandni Patel,[1] Emma Armstrong,[1] Kathryn Costelloe,[1] Lorenza Magno,[1] Magda Bictash,[1] E. Yvonne Jones,[2] Paul V. Fish,[1,*] Fredrik Svensson[1,*]

[1] Alzheimer's Research UK UCL Drug Discovery Institute, University College London, The Cruciform Building, Gower Street, London, WC1E 6BT, U.K.

[2] Division of Structural Biology, Wellcome Centre for Human Genetics, University of Oxford, The Henry Wellcome Building for Genomic Medicine, Roosevelt Drive, Oxford, OX3 7BN, U.K.

Abstract

Notum is a negative regulator of Wnt signaling acting through hydrolysis of a palmitoleoylate ester, which is required for Wnt activity. Inhibitors of Notum could be of use in disease where dysfunctional Notum activity is an underlying cause. A docking-based virtual screen (VS) of a large commercial library was used to shortlist 952 compounds for experimental validation as inhibitors of Notum. The VS was successful with 31 compounds having an IC_{50} <500 nM. A critical selection process was then applied with two clusters and two singletons (**1-4d**) selected for hit validation. Optimization of **4d** guided by structural biology identified potent inhibitors of Notum activity that restored Wnt/β-catenin signaling in cell-based models. The [1,2,4]triazolo[4,3-*b*]pyradizin-3(2*H*)-one series **4** represents a new chemical class of Notum inhibitors and the first to be discovered by a VS campaign. These results demonstrate the value of VS with well-designed docking models based on X-ray structures.

Key words: hit-finding; Notum inhibitors; [1,2,4]triazolo[4,3-*b*]pyradizin-3(2*H*)-ones; structural biology; virtual screening; Wnt signaling.

INTRODUCTION

Notum is a secreted carboxylesterase that catalyzes the depalmitoleoylation of Wnt proteins and, by doing so, acts as a negative regulator of Wnt signaling.[1,2] Inhibitors of Notum activity are becoming valuable research tools to help determine the role Notum performs in human disease.[3,4] There have been several reports of small molecule Notum inhibitors discovered by the application of a variety of hit-finding approaches, including: high-throughput screening,[5,6] activity-based protein profiling,[7] fragment screening,[8-11] and scaffold-hopping.[12] There has been extensive structural characterization of Notum with known lipid-protein substrates Wnt[1] and ghrelin[13] providing a detailed understanding of the mechanism of hydrolysis. In addition, many of these inhibitors have had their Notum binding modes determined by crystallography[8-12] and so there is ample structural information available in the Protein Data Bank (PDB).[14]

The Notum structures show a defined, hydrophobic active-site pocket that accommodates the palmitoleate (C16) group of Wnt, and n-octyl (C8) group of ghrelin, located next to the catalytic triad (Ser232, His389, Asp340). Most inhibitors bind within this active-site pocket,[3] although some show significant variation in position or orientation of the ligands even between close analogues.[8,15] The combination of this druggable pocket[16,17] with high quality structural information identified Notum as an ideal candidate for a docking-based virtual screening campaign supported by structure-based drug design (SBDD). Indeed, we have previously demonstrated the use of docking combined with SBDD to guide compound optimization for Notum fragment screening hits.[8,10,11]

Virtual screening (VS) is well-established for hit-finding, with a number of proven methods described in the literature.[18,19] It was considered that a VS campaign could discover new chemical matter in a rapid, cost-efficient manner and investigate a new hit-finding strategy for Notum. Validated hits could then be optimized with the objective of delivering structurally orthogonal leads for use in disease models to establish target validation. Here, we describe the application of docking-based VS to identify novel Notum

inhibitors. Several hit series are discussed and the most promising, [1,2,4]triazolo[4,3-b]pyradizin-3(2H)-ones **4**, was further developed as a novel Notum lead series.

RESULTS AND DISCUSSION

Due to the rich structural information available for Notum, we elected to conduct a VS based on docking. In this Article, we present our process and results from VS of a commercial chemical library through to the identification, validation and optimization of potent inhibitors of Notum activity that were evaluated in mouse pharmacokinetic (PK) experiments (**Figure 1**).
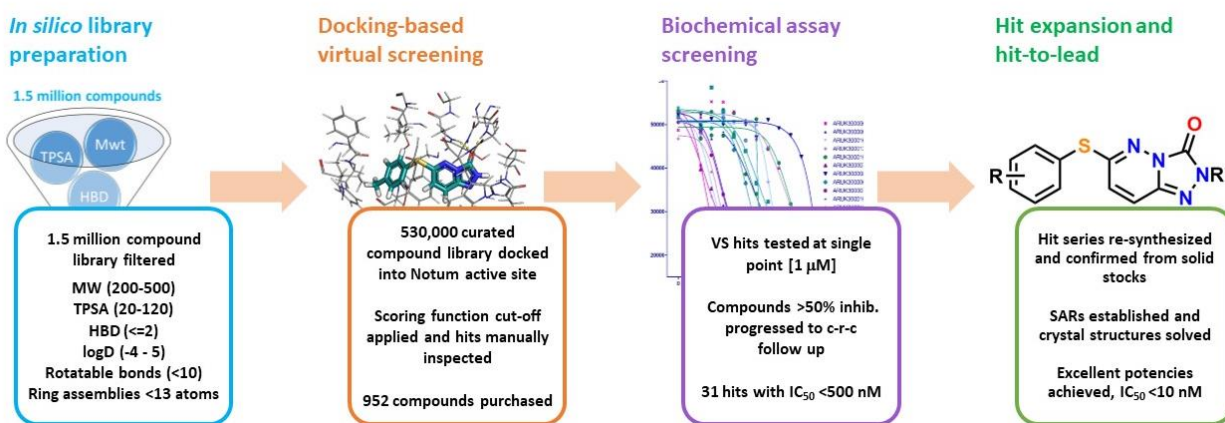

Figure 1. Flow diagram of the virtual screening campaign.

Virtual Screening

It has been our experience that it is beneficial to select a commercial screening library from a single vendor to simplify procurement.[19] The full ChemDiv (San Diego CA, US) library (ca. 1.5 million compounds) was chosen for the VS.[20] The library was filtered for desirable chemical properties (MW, TPSA, HBD, clogD, NRB) and the remaining 534,804 compounds were screened *in silico* using Glide (details in the Experimental Section).[21,22] Of these, 1330 compounds had an excellent docking score of -9 or better. Based on these docking results and a manual inspection of the 'virtual hits', 1088 compounds were short-listed for purchase of which 952 were available and could be ordered from the supplier.[20] At this early point in

the filtering process, we selected to retain a small proportion of compounds that may be perceived as PAINs[23] and/or Structural Alerts[24] as we wished to give ourselves the opportunity to discover compounds that could act as soft electrophiles, e.g. esters, enoates.[25] These compounds could act as a new class of covalent inhibitors of Notum through reaction with the catalytic Ser232.[7]

Hit identification

The 952 purchased compounds were screened in a Notum biochemical assay as previously described.[8,10] In brief, test compounds were incubated with human Notum (81-451 Cys330Ser) and trisodium 8-octanoyloxypyrene-1,3,6-trisulfonate (OPTS) as the substrate for 40 min, and fluorescence measured. A direct inhibitor of Notum (IC$_{50}$) would suppress fluorescence by binding in the catalytic pocket of Notum and preventing hydrolysis of OPTS.[8,10]

The compounds were initially screened at two single point concentrations of 1 and 10 μM (n = 2). Overall, 44 compounds showed an average inhibition >50% at 1 μM (hit rate 4.6%), and 158 compounds >50% at 10 μM (hit rate 16.6%), from the VS (**Figure S1**). This preliminary hit rate is consistent with other successful VS campaigns reported in the literature.[19,26] The data set has been made available as Supporting Information.

All compounds exhibiting single point inhibition >50% at 1 μM were then screened in 10-point concentration-response curve mode (30 pM to 10 μM). Thirty-one compounds had an IC$_{50}$ <500 nM, which consisted of four clusters of structurally similar compounds along with eight singletons (hit rate 3.2%) (structures of these 31 hits are available in **Figure S2**).

Hit selection

These 31 hits were then critically reviewed based on standard drug-like criteria along with their potential for further optimization to improve potency and build in good ADME properties. At this point,

compounds and clusters were also deselected due to their potential for assay interference, overt reactivity, or structural similarity to known inhibitors of Notum. In addition, the single point data was revisited to identify any close analogues that were weakly active/inactive (<50% inhib. @ 1 μM) to provide preliminary structure-activity relationships (SAR).

Clusters and singletons to be deselected included: 7H-furo[3,2-g]chromen-7-ones (4 examples), 3-acyl-9H-carbazoles (5 examples), perimidin-2-ones (1 example) and various polyenes (4 examples); these represented 14 of the 31 hits.

An additional four singletons were placed on hold with the view that they could be revisited should the need arise. These compounds were neither flawed nor particularly attractive; we simply opted to invest our first efforts in alternative templates.

The preferred hits included two clusters (**1**, **2**) and two singletons (**3**, **4d**), which were selected for hit validation and expansion (**Figure 2**).
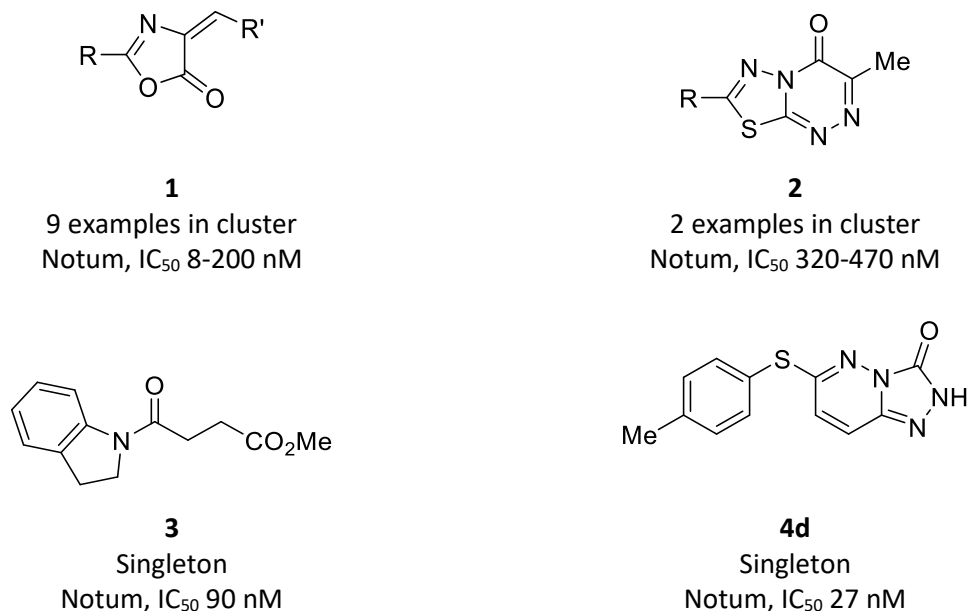
1
9 examples in cluster
Notum, IC$_{50}$ 8-200 nM

2
2 examples in cluster
Notum, IC$_{50}$ 320-470 nM

3
Singleton
Notum, IC$_{50}$ 90 nM

4d
Singleton
Notum, IC$_{50}$ 27 nM

Figure 2. Original VS hits selected for hit validation and expansion.

Three of these four hits had the *potential* to act as covalent inhibitors of Notum with varying degrees of reactivity and reversibility (**1**, Michael acceptor; **3**, acylation via ester; **4d**, thioether as leaving group). This potential for reactivity was investigated during the hit validation process, initially through a search of relevant published literature, followed by experimental assessment if justified (*vide infra*).

Hit validation and lead expansion

Notum inhibition of these hits was then confirmed in the Notum (OPTS) biochemical assay (IC_{50}) with solid material, which was either purchased or synthesized. In addition, these hits were submitted for structural studies by soaking in Notum crystals and X-ray structure determination. Preferred compounds were screened in a cell-based TCF/LEF (Luciferase) reporter assay to measure their ability to restore Wnt/β-catenin signaling when activated by exogenous recombinant WNT3A in the presence of Notum. An inhibitor of Notum should show an activation of Wnt signaling (EC_{50}).[8,10] Selected inhititors were then assessed *in vitro* in ADME assays (solubility, microsomal stability, cell permeability) to establish suitability for progression to *in vivo* mPK studies.

A brief description of these activities is presented for the VS hits **1**-**3** followed by a more detailed discussion of the [1,2,4]triazolo[4,3-*b*]pyradizin-3(2*H*)-ones **4**.

4-Benzylidene-2-phenyloxazol-5(4H)-ones (1)

Oxazol-5(4*H*)-ones **1** are versatile heterocycles that have shown a wide range of pharmacological activities.[27] They are also useful synthons for the preparation of unnatural amino acids and isomerization of their Z- to E-geometry can be used, in principle, as molecular photoswitches.[28]

Eight oxazolones **1** showed Notum activity with IC_{50} <200 nM and all had been assigned the *E*-configuration as purchased (**Table 1**). One compound (**1i**) was removed from the original hit set as it

showed a variable response. The identification of inhibitors with excellent biochemical potency straight out of the VS prompted rapid evaluation through the screening sequence.

Synthetic methods to prepare *E*-oxazolones were not readily available, whereas routes to the corresponding *Z*-oxazolones are generally reported by application of the classical Erlenmeyer-Plöchl synthesis.[28,29] Original hits **1c** and **1f** were synthesized as the corresponding *Z*-isomers, **1j** and **1k** respectively, by an acid-catalyzed condensation of the formamidoacetic acid (**5**) and aldehyde (**6**) reactant pair (**Scheme 1**). Docking of both *E* and *Z* isomers showed that the docking model strongly preferred the *E* isomer (**Figure S4**), however, screening data displayed very similar activity for these two matched pairs.

Evaluation of **1f** and **1k** in the Notum TCF/LEF assay showed very weak activity (EC$_{50}$ >10 µM), and this disconnection was reproduced by additional oxazolones, including more polar analogues (**Table S11**). A representative set of oxazolones, including **1k**, were also screened *in vitro* ADME assays. Most had poor aqueous solubility (≤0.3 ug/mL) and all showed negligible cell permeability as measured across a MDCK-MDR1 cell monolayer. They did demonstrate very high metabolic stability in mouse liver microsomes (MLM). (Details in the Supporting information, **Tables S1-S6**).

The 4-benzylidene oxazol-5(4*H*)-one template **1** can undergo a variety of chemical reactions including acting as a Michael acceptor with S, N and C nucleophiles, albeit at elevated temperatures.[30] However, we did not observe any reactivity with Notum, although this was not specifically investigated.
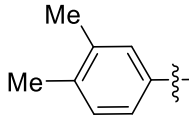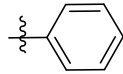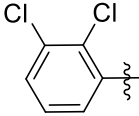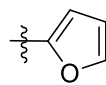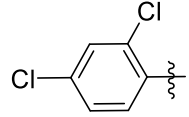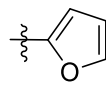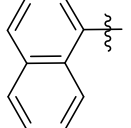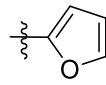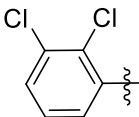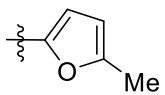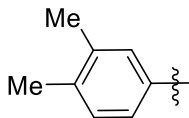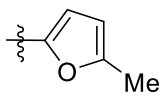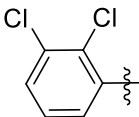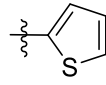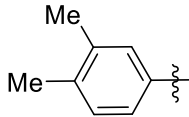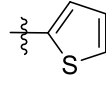
These compounds, and the cluster in general, exhibited the hallmarks of a 'problem series'. As their insolubility was related to the extended aromatic nature and high lipophilicity, an extensive redesign to improve solubility was unlikely to retain Notum activity. Hence, this cluster was not investigated any further.
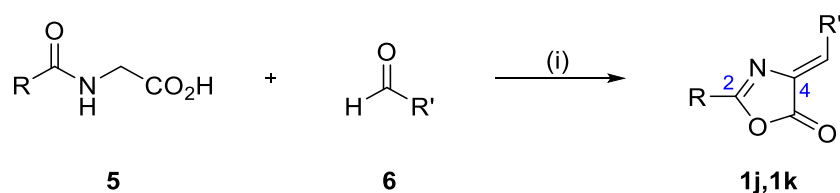
Scheme 1. Synthesis of (*Z*)-oxazol-5(4H)-ones (**1**). Reagents and conditions: (i) Formamidoacetic acid **5** (1.0 equiv.), aldehyde **6** (1.0 equiv.), NaOAc (1.0 equiv.), Ac$_2$O, 140 °C, 2 h.

Table 1. Notum inhibition for *E*- and *Z*-oxazolones **1**. [a,b]

1a-1i   1j,1k

Compound	R	R'	Notum IC$_{50}$ (nM)
E-oxazolones:			
1a	Me, Me (dimethylphenyl)	phenyl	200
1b	Cl, Cl (dichlorophenyl)	furan	12
1c	Cl, Cl (dichlorophenyl)	furan	48
1d	naphthyl	furan	100
1e	Cl, Cl (dichlorophenyl)	Me-furan	22
1f	Me, Me (dimethylphenyl)	Me-furan	8.5
1g	Cl, Cl (dichlorophenyl)	thiophene	54
1h	Me, Me (dimethylphenyl)	thiophene	24

1i	Cl, Cl (dichlorophenyl)	MeO, OMe (dimethoxyphenyl)	c

Z-oxazolones:

1j	Cl, Cl (dichlorophenyl)	furan (O)	14
1k[d]	Me, Me (dimethylphenyl)	Me-furan (O)	17

[a] IC_{50} and EC_{50} values presented in text and Tables refer to the Notum OPTS and TCF/LEF assays respectively, unless stated otherwise.

[b] All values are mean of n = 2-8 experiments quoted to 2 s.f. Differences of <2-fold should not be considered as significant.

[c] **1i** showed a significant drop-off in activity upon retest (IC_{50} > 10 µM) and, retrospectively, a variable response in the single point data.

[d] In vitro ADME data for **1k**: aqueous solubility, 0.31 µg/mL; MLM, Cl_i 1.9 µL/min/mg protein, $T_{1/2}$ 360 min; MDCK-MDR1, AB/BA P_{app} 0/0 x10^{-6} cm/s, with poor recovery (<25%).

*[1,3,4]Thiadiazolo[2,3-c][1,2,4]triazin-4-ones (**2**)*

Two thiadiazolotriazinones hits highlighted this chemotype as a high scoring scaffold from the VS. An additional seven examples showed Notum inhibition with 4-43% inhibition at 1 µM (Supporting Information). They were of particular interest as they represented a novel chemical motif not previously described as inhibitors of Notum. Analysis of the docking poses of **2a** and **2b** showed the head-group bound in the entrance to the active site, with the carbonyl oxygen atom residing in the oxyanion hole, and the pendant aryl ring in the hydrophobic pocket (**Figure 3**).
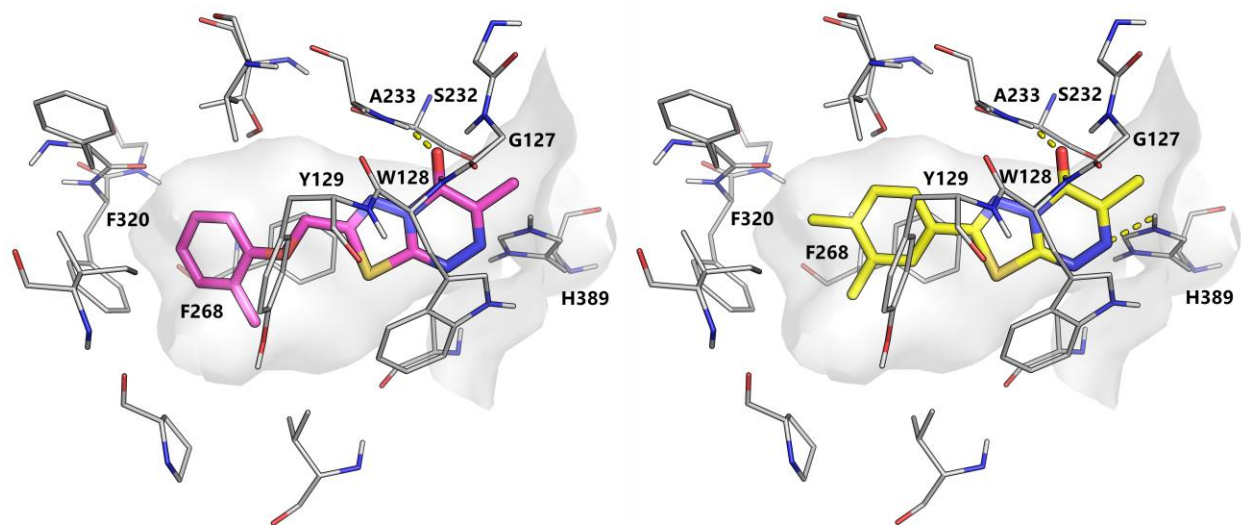
Figure 3. Docking poses (using 6T2K) for VS hits **2a** (pink) and **2b** (yellow). **2a** forms an interaction with Ala233, whereas **2b** with Ala233 and His389. Select binding site residues shown within 4Å of their respective ligands. Polar contacts are indicated as dashed lines. Water molecules have been removed for clarity. The surface of the Notum binding pocket outlined (gray) from the docking receptor (6T2K). For full human Notum active site residue numberings, see **Figure S3**.

Authentic samples of inhibitors **2a** and **2b** were resynthesized via a condensation of 1,2,4-triazine-5(4*H*)-one (**8**) with the required carboxylic acid **7** to confirm Notum activity from solid material (**Scheme 2**, **Table 2**). However, the Notum activity, as assessed by IC$_{50}$ values, for the resynthesized materials were 5 – 12-fold weaker than measured for the original library liquid stocks. The solid materials also had limited solubility. This series was halted.
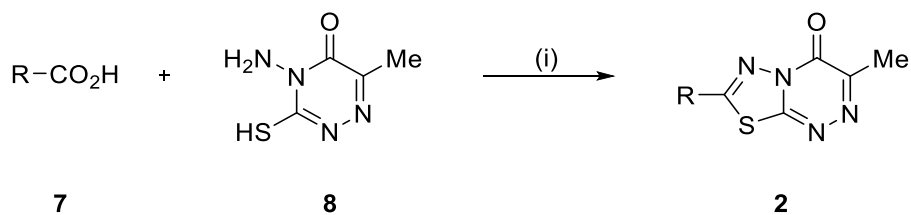
Scheme 2. Synthesis of thiadiazolonetriazoles. Reagents and conditions: (i) $POCl_3$ (excess), 4-amino-3-mercapto-6-methyl-1,2,4-triazine-5($4H$)-one (**8**) (1 equiv.), RCO_2H **7** (2 equiv.), 90 °C, 1 h.

Table 2. Notum inhibition for thiadiazolonetriazoles **2a** and **2b**.[a]

Compound	R	Notum IC_{50} (nM)
2a	Me (2-methylbenzyl ether)	320[b] 1600[c]
2b	Me, Me (3,4-dimethylphenyl)	470[b] 5600[c]

[a] See footnotes in **Table 1**.
[b] value measured from original liquid stock.
[c] value measured from solid material.

*Methyl 4-(indolin-1-yl)-4-oxobutanoate (**3**)*

A high-resolution crystal structure of the Notum inhibitor **3** complex revealed that a covalent adduct had formed between Ser232 of the catalytic triad and the oxobutanoate ester (PDB: 7ARG). The covalent interaction was confirmed by mass-spectrometry analysis and was shown not to form with the Notum S232A mutant. These detailed mechanistic studies have been published separately in this journal.[31]

*[1,2,4]Triazolo[4,3-b]pyradizin-3(2H)-ones (**4**)*

Several compounds with a triazolopyradizinone core were identified from the VS as having good docking scores. Analysis of the docking pose of the single VS hit **4d** (IC_{50} 27 nM, pIC_{50} 7.6) showed the triazolopyradizinone head-group bound in the entrance to the active site, with the carbonyl oxygen

occupying the oxyanion hole, and the lipophilic group extending deeper into the pocket, linked by a thioether (**Figure 4**). Compound **4d** was resynthesized by a microwave-assisted nucleophilic aromatic substitution (**Scheme 3**) and confirmed as an inhibitor of Notum catalyzed OPTS hydrolysis. Evaluation of **4d** by standard design metrics confirmed good physicochemical properties (MW 258, clog*P* 1.9, TPSA 57, HAC 18), efficient binding (LE 0.59; LLE 5.7), and potential for brain penetration as assessed by CNS MPO calculation (5.7/6.0)[32] and BBB score (4.2/6.0).[33]
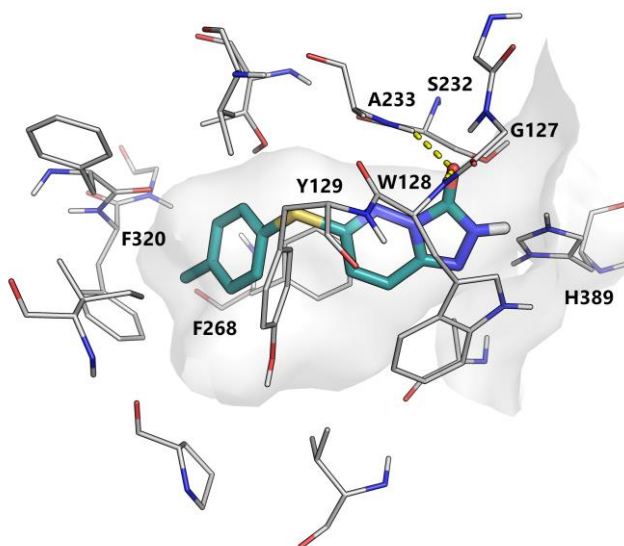
Figure 4. Docking pose for VS hit **4d** (teal, using 6T2K). The compound forms potential hydrogen bonds with the backbone of Ala233 and Trp128. For details shown in the figure, see Figure 3.
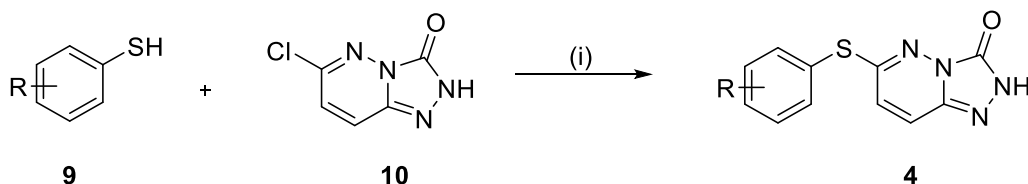
Scheme 3. Microwave assisted synthesis of triazolopyradizinones **4**. Reagents and conditions: (i) ArSH (**9**) (1.0 equiv.), 6-chloro-[1,2,4]triazolo[4,3-*b*]pyridazin-3(2*H*)-one (**10**) (1.0 equiv.), Cs$_2$CO$_3$ (1.0 equiv.), DMF, 150 °C, microwave, 30 min.

The 6-phenylsulfanyl triazolopyradizin-3(2*H*)-one template **4** is novel in the chemical literature and it was encouraging that throughout the course of the experiments reported herein, **4** displayed no evidence of reactivity with Notum or hydrolytic instability.

*Development of triazolopyradizinones (**4**) as a novel Notum lead series*

Retrosynthesis of **4d** into its triazolopyradizinone head-group and aryl thiol components guided our initial strategy as inhibitors were readily prepared using this established synthetic methodology. New inhibitors were designed to further improve potency by optimal occupancy of the hydrophobic pocket, and to build in good ADME properties and/or remove ADME liabilities. SARs were initially directed towards optimization of the aryl ring **4a-4gg** with the unsubstituted phenyl **4a** prepared as the benchmark to assess these changes (**Table 3**).

Table 3. Notum inhibition for triazolopyradizinones **4a-4gg.** SAR of aryl ring.[a]
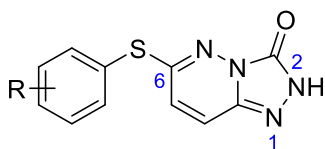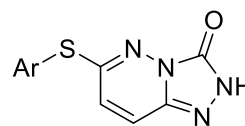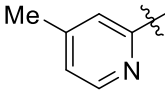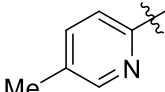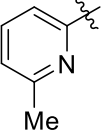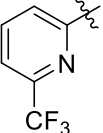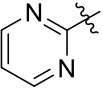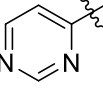
	4a-4aa		**4bb-4gg**

Compound	R or Ar	Notum (OPTS) IC$_{50}$ (nM)	Notum (TCF/LEF) EC$_{50}$ (nM)
4a	H	150	nd[b]
4b	2-Me	50	300
4c	3-Me	9	240
4d (hit)	4-Me	27	480
4e	2-Cl	30	720

4f	3-Cl	6	88
4g	4-Cl	21	310
4h	2-F	87	1100
4i	3-F	30	260
4j	4-F	94	540
4k	2-CF$_3$	89	930
4l	3-CF$_3$	17	190
4m	4-CF$_3$	28	300
4n	3-OMe	15	140
4o	3-OEt	20	150
4p	3-OCF$_3$	4	34
4q	3-OiPr	25	260
4r	3-SMe	24	380
4s	2-Me,3-Me	14	nd
4t	2-Me,4-Me	27	300
4u	3-Me,4-Me	7	130
4v	3-Me,5-Me	47	nd
4w	2-Cl,3-Cl	13	150
4x	2-Cl,4-Cl	20	380
4y	3-Cl,4-Cl	5	110
4z	2-F,3-F	63	nd
4aa	3-F,4-F	120	1100
4bb	Me-substituted pyridine (4-Me)	2,700	nd
4cc	Me-substituted pyridine (5-Me)	3,600	nd

4dd	(2-pyridyl, 6-Me)	650	>10,000
4ee	(2-pyridyl, 6-CF$_3$)	410	>10,000
4ff	(2-pyrimidinyl)	>10,000	nd
4gg	(4-pyrimidinyl)	>10,000	nd

[a] See footnotes in **Table 1**.

[b] nd, not determined

Many analogues were identified as potent inhibitors of Notum (IC$_{50}$ <50 nM) with five examples (**4c, 4f, 4p, 4u, 4y**) having activity superior to the original hit (IC$_{50}$ <10 nM). A wide range of small, lipophilic substituents were tolerated on the phenyl ring, with a general trend that substitution at the 3-position was preferred: 3-position > 4-position ≥ 2-position; this trend was observed for the Me, Cl, F and CF$_3$ groups. The 3-position was therefore chosen for further investigation, and a range of larger lipophilic substituents were well tolerated, e.g. 3-OCF$_3$ **4p** (IC$_{50}$ 4 nM). Disubstitution of the phenyl ring was also well tolerated and again a trend was observed that combinations of 3,4-substitution were generally favored over combinations which included a 2-substituent (e.g. 3-Me,4-Me **4u** vs 2-Me,4-Me **4t**). Attempts to introduce polarity into the hydrophobic pocket through the application of heterocycles as replacements for the phenyl ring were not successful **4bb-4gg**, even when combined with preferred groups at the *meta*-position (**4dd**, **4ee**).

These initial SARs established the triazolopyradizinones **4** as a promising lead series for further development.

To investigate the binding modes of the triazolopyradizinones, and to validate the docking model, selected inhibitors were chosen for characterization by X-ray crystallography. This series proved to be very amenable to crystallization by soaking and eight structures were solved with inhibitors bound to Notum in the active site (**Figure 5, Table S12**).

4c: R = 3-Me	**4d**: R = 4-Me
4e: R = 2-Cl	**4f**: R = 3-Cl
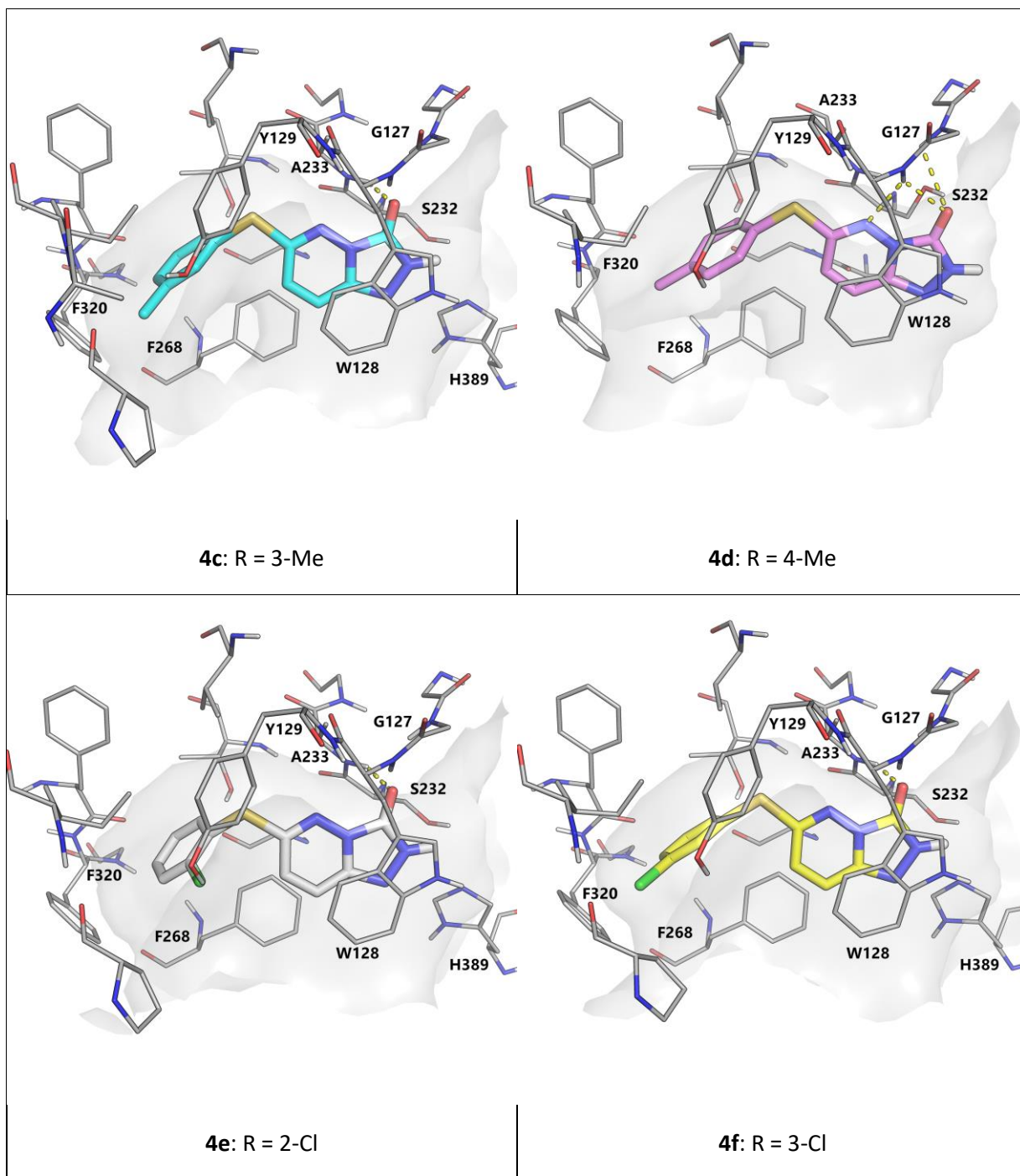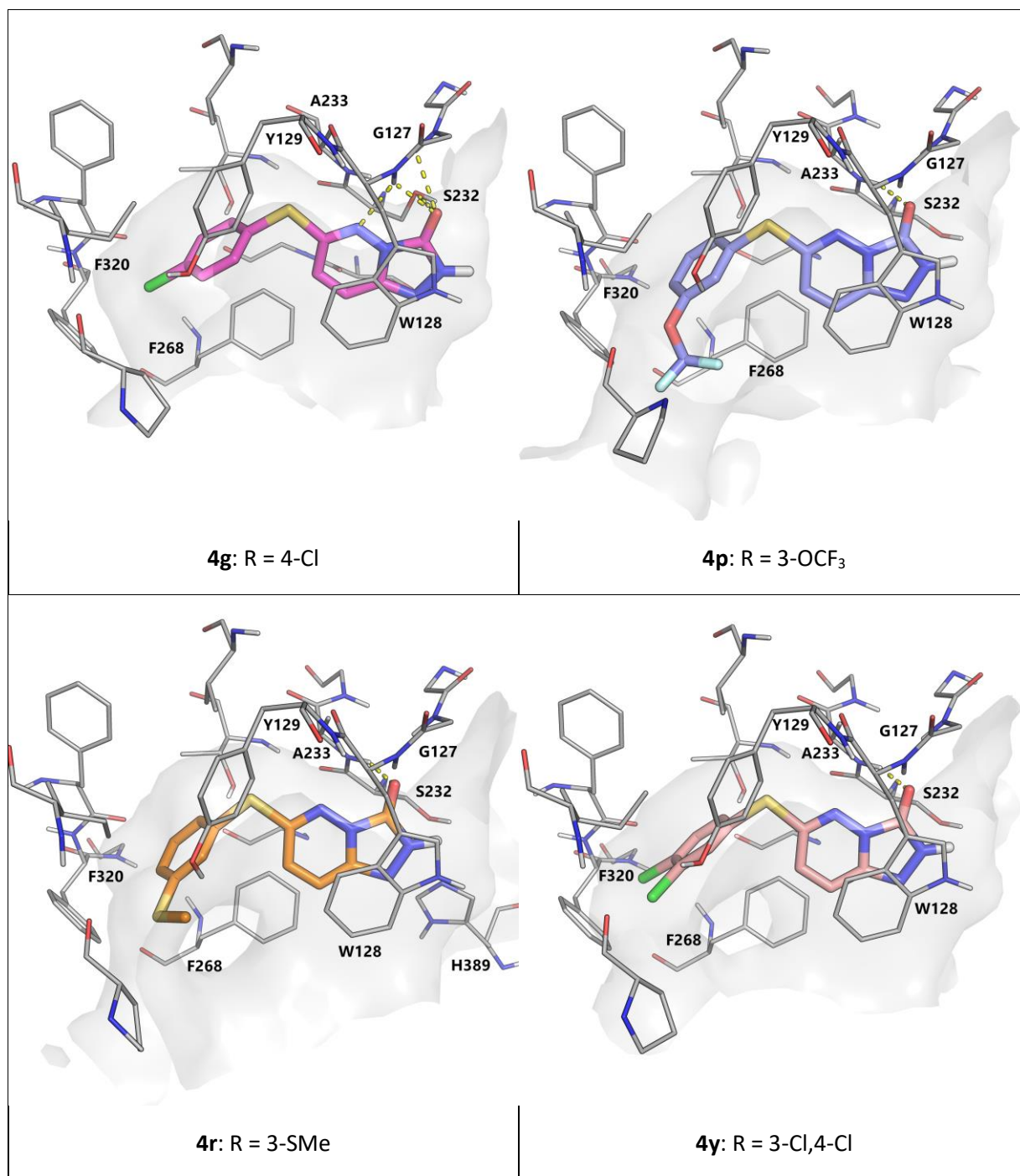
Figure 5. X-ray structures of triazolopyradizinones. The aryl substituent (R) is defined for clarity. PDB codes in parenthesis: **4c** (7B3X), **4d** (7B4X), **4e** (7B3G), **4f** (7B3I), **4g** (7B3P), **4p** (7B3H) and **4r** (7B45), **4y** (7B50). Pocket outlines (gray) are based on the respective structures. For other details shown in the figure, see Figure 3.

Comparing the binding pose generated by Glide for **4d** with the X-ray structure reveals a close match with the overall positioning of the compound in close agreement (**Figure 6**). The only notable difference is that in the crystal structure the ligand is positioned slightly further out of the pocket resulting in a different hydrogen bond pattern with the oxyanion hole compared to the docked pose. However, crystal structures of other analogues reveal a binding mode very close to that predicted for **4d**. This can possibly be explained by *para* substitution pushing the compound further out of the pocket as the same binding for **4d** is observed for **4g**, although not for **4y**.
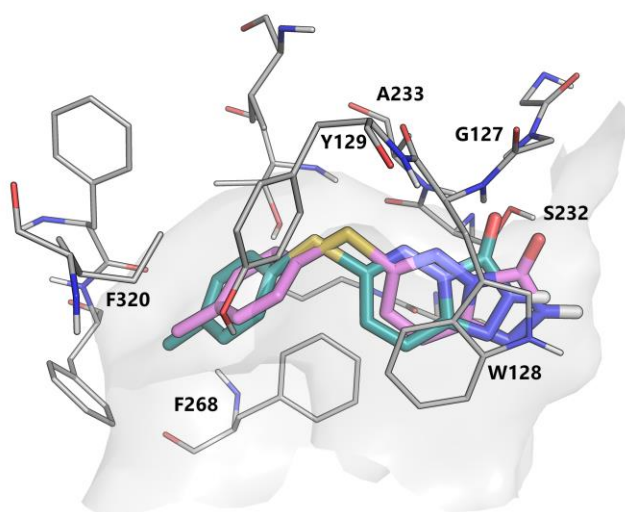
Figure 6. Overlay of x-ray crystal structure (pink, 7B4X) and docking pose (teal, using 6T2K) for **4d**. Pocket outlined (gray) from 7B4X. For other details shown in the figure, see Figure 3.

Additional SAR investigation of the linker and substitution of the triazolopyradizinone head-group failed to identify any groups that offered an advantage, in fact, these changes were detrimental to Notum activity (**Table 4**, **Schemes 4-7**). The original thioether linker was found to be superior to alternatives with a reduction in activity in the order $S > CH_2 > NH \geq NMe > O > SO \approx SO_2$. Limited SAR by substitution of the head-group was restricted to methylation at the R^7, R^8 and NR^2 positions. Mono methylation at R^8 **4nn**

gave a modest 2.6-fold decrease compared to the hit **4d**, whereas dual methylation at R^7 and R^8 **4oo**

significantly reduced activity. These results suggest there is some scope for substitution at the R^8 position

and this was supported by the binding model where there is sufficient space to accommodate a methyl

group. Methylation at N2 of **4d** as **4pp** abolished activity (25-40% inhib. @ 10 μM) suggesting that

ionization was required for activity.[34] Additional head-group modifications were not investigated.
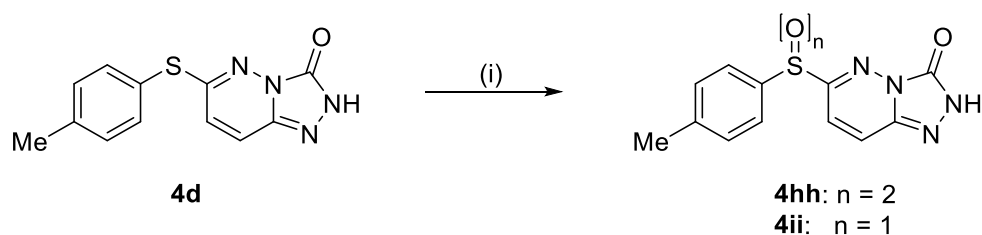
Scheme 4. Oxidation of thioether **4d** to **4hh** and **4ii**. Reagents and conditions: (i) OXONE (3.9 equiv.), DMF, RT, microwave, 18 h.
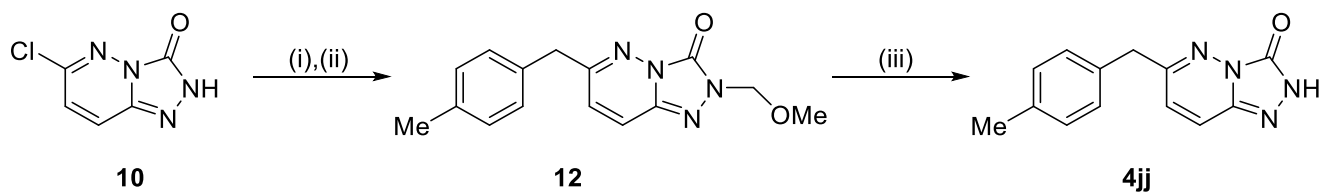
Scheme 5. Reagents and conditions: (i) MeOCH₂Cl (2.0 equiv.), NEt₃ (3.9 equiv.), DMF, RT, 72 h; (ii) Pd(OAc)₂ (0.1 equiv.), XPhos (0.2 equiv.), 4-methylbenzyl zinc chloride (2.0 equiv.), THF, RT to 65 °C, 18 h; (iii) TFA (excess), 55 °C, 18 h.
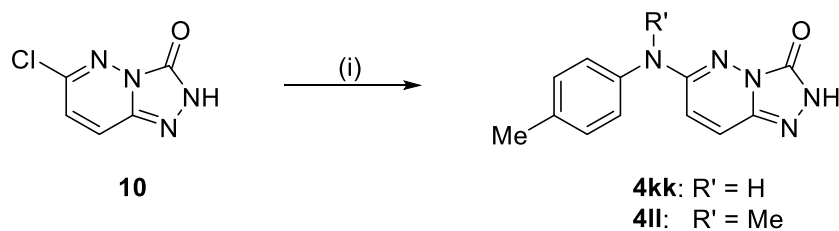
Scheme 6. Reagents and conditions: (i) p-TsOH.H₂0 (1.2 equiv.), 4-TolNHR' (1.0 equiv.), n-BuOH, 180 °C, microwave, 16 h.

Scheme 7 (structures):
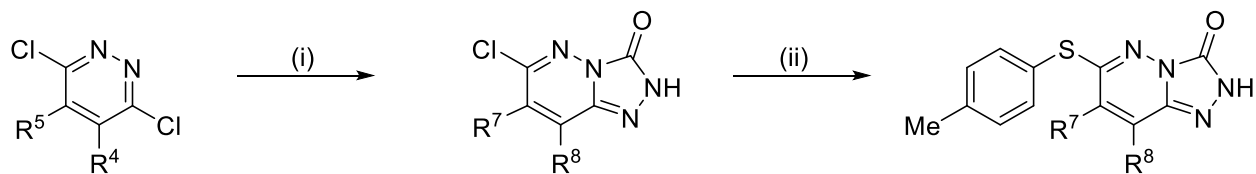
13a: R^4 = Me; R^5 = H
13b: R^4 = R^5 = Me

(i) →

14a: R^7 = H; R^8 = Me
14b: R^7 = R^8 = Me

(ii) →

4nn: R^7 = H; R^8 = Me
4oo: R^7 = R^8 = Me

Scheme 7. Reagents and conditions: (i) $H_2NC(=O)NHNH_2 \cdot HCl$ (2.0 equiv.), conc. HCl (0.08 equiv.), EtOH, 85 °C, 72 h; (ii) 4-TolSH (1.0 equiv.), Cs_2CO_3 (1.0 equiv.), DMF, 150 °C, microwave, 30 min.

Table 4. Notum inhibition for triazolopyradizinones **4hh-4pp.** SAR of the linker (X) and head-group (NR^2, R^7, R^8).[a]

4hh-4pp (structure)
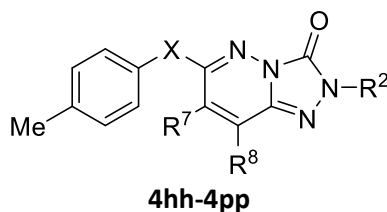
Compound	X	R^2	R^7	R^8	Notum (OPTS) IC_{50} (nM)
4d (hit)	S	H	H	H	27
4hh	SO_2	H	H	H	>10,000
4ii	SO	H	H	H	>10,000
4jj	CH_2	H	H	H	240
4kk	NH	H	H	H	690
4ll	NMe	H	H	H	990
4mm	O	H	H	H	3100
4nn[b]	S	H	H	Me	70
4oo	S	H	Me	Me	>10,000
4pp	S	Me	H	H	>10,000

[a] See footnotes in **Table 1**.
[b] **4nn** was prepared as predominantly the 8-Me isomer but contained a small amount of the 7-isomer, 8-Me:7-Me, 5:1.

Throughout the design cycle selected Notum inhibitors were evaluated for their ability to activate Wnt

signaling in a more physiologically relevant context. There was a good correlation between activity in the

biochemical (OPTS substrate) assay with activity in the TCF/LEF assay (WNT3A substrate), albeit with a ~10-fold decrease in potency in the cell-based system (**Table 3**, **Figure S5**). All inhibitors tested that demonstrated IC_{50} <100 nM in the OPTS assay, showed consistently good activities in the TCF/LEF assay.

Hit **4d** and preferred inhibitors **4f**, **4p** and **4y** were then revaluated in the TCF/LEF assay in more detail under slightly modified experimental conditions (see Experimental Section). All four robustly restored Wnt signaling in the presence of Notum (EC_{50} <100 nM; n = 3) (**Table 5**) and gave standard S-shaped concentration-response curves with a maximal response at the highest concentration tested (10 µM); there was no evidence of supra- or submaximal responses. Performing these experiments in the absence of Notum showed a maximal Wnt response at all concentrations of compounds tested (up to 10 µM; n = 3). In addition, **4d**, **4f**, **4p** and **4y** showed no adverse effects on cell health (as assessed by Cell Titre Glo assay; n = 5) or total cell number (as measured by GFP; n = 2) in the presence and absence of Notum (up to 10 µM). These results confirm that the activation of Wnt signaling was due to on-target inhibition of Notum activity and not caused by assay interference or cell toxicity (up to 10 µM).

Table 5. Summary of Notum inhibition for **4d, 4f, 4p** and **4y**.[a] Comparison with LP-922056.
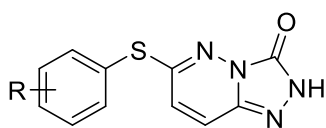
4d: R = 4-Me
4f: R = 3-Cl
4p: R = 3-OCF$_3$
4y: R = 3-Cl,4-Cl
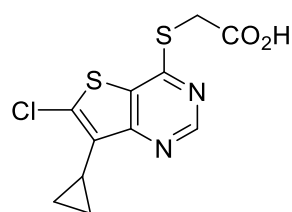
LP-922056

	4d (hit)	**4f**	**4p**	**4y**	**LP-922056** [b]
PDB	7B4X	7B3I	7B3H	7B50	6T2K
Notum IC_{50} (nM)	27 ± 14 (n = 8)	6.3 ± 0.5 (n = 4)	4.5 ± 1.4 (n = 4)	5.5 ± 1.6 (n = 4)	1.1
Notum EC_{50} (nM)[c]	86 ± 54 (n = 3)	37 ± 6 (n = 3)	10 ± 0.4 (n = 3)	29 ± 6 (n = 3)	23
clog$P$	1.9	2.2	2.4	2.7	3.1

^a See footnotes in **Table 1**.

^b Values taken from references 3, 6 and 12.

^c These values were generated under slightly modified experimental conditions compared to **Table 3**, see Experimental Section.

A few potent Notum inhibitors showed excellent activity in both Notum inhibition assays supported by structural information, i.e. **4f**, **4p** and **4y**. These three inhibitors, along with the original hit **4d**, were then assessed in mPK experiments to determine their suitability as *in vivo* chemical tools.

ADME properties and mouse pharmacokinetics for **4**.

The original VS hit **4d** was selected for further study in ADME assays as a representative example from this series. This early lead **4d** has properties consistent with small molecule lead-like drug space (**Table 6** and **Tables S1-S8**). The N2 proton of the triazolopyradizin-3(2*H*)-one of **4d** is weakly acidic with a measured pK_a of 7.9 (ca. 24% ionized at physiological pH 7.4). The pK_a value was encouraging as weakly acidic compounds can have a profound influence upon brain penetration.[10,35] Compound **4d** demonstrated moderate/high metabolic stability in MLM, high permeability in a MDCK-MDR1 assay with minimal P-gp mediated efflux (ER = 0.83), and high binding to mouse plasma proteins resulting in a low free drug fraction (f$_u$ 0.011).

Table 6. Summary of properties of **4d**.^a

	4d
Physicochemical and molecular properties	
mol wt	258
clog*P*	1.9
TPSA (Å^2)	57
pK_a	7.9
CNS MPO	5.7/6.0
BBB score	4.2/6.0
Notum inhibition	
OPTS, IC$_{50}$ (nM)	27 ± 14 (n = 8)
TCF-LEF, EC$_{50}$ (nM)	86 ± 54 (n = 3)

ADME profile

Aq. solubility (µg/mL)/(µM)	32/120
Mouse plasma protein binding (PPB) (%)	98.9
MLM, Cl_i (µL/min/mg protein)	21
MDCK-MDR1, AB/BA P_{app} (x10^{-6} cm/s)	52/43
MDCK-MDR1, efflux ratio (ER)	0.83

[a] See footnotes **Table 1.**

Pilot pharmacokinetic data for **4d, 4f, 4p** and **4y** was performed in mouse with a cassette dosing regimen to measure plasma and brain exposure (**Table 7, Tables S9-S10** and **Figure S6**). A single intravenous (i.v.) dose of 0.4 mg/kg showed all compounds to have a modest half-life. The plasma clearance (CL) was low/moderate as typically <20% of liver blood flow (LBF), however, the volumes (Vd_{ss}) were low indicating minimal distribution into tissues. All compounds had negligible brain levels at the two measured time points (1 and 4 hr).[36] However, these studies are somewhat confounded as steady state is unlikely to have been achieved with single acute dosing.

Some outcomes of these *in vivo* PK experiments were unexpected based upon the compound's physicochemical properties and the *in vitro* ADME data. Original hit **4d** is weakly acidic and yet it has a PK profile more consistent with that of a carboxylic acid (high PPB, high unbound CL, low Vd and low BBB penetration). The disconnection between high permeability in the MDCK-MDR1 cell assay and the poor BBB penetration observed *in vivo* may be due to recognition of **4d** by BBB efflux transporters other than P-gp such as the BCRPs and MRPs that export anionic substrates.[37] The poor correlation between these *in silico*, *in vitro* and *in vivo* models for BBB permeability of weak acids has been previously observed by us,[10] and suggests that an early assessment of a fit-for-purpose lead in rodent PK experiments would be prudent.

Based on these profiles, additional PK studies were not justified and our efforts have been directed towards the redesign of the head-group to improve the PK profile and, ideally, introduce BBB permeability so the tools could have utility in models of neurodegenerative disease. Our redesign strategy was to retain

the [6,5]-heterocyclic headgroup, as this seemed to confer good Notum activity when combined with a pendant aryl ring, whilst removing acidic protons and attenuating hydrogen bonding capacity to improve BBB permeability.

Table 7. Mouse pharmacokinetic data for **4d, 4f, 4p** and **4y** by cassette intravenous dosing.[a]

Compound	4d	4f	4p	4y
Plasma PK Parameters, i.v. (mean):				
Dose (mg/kg)	0.4	0.4	0.4	0.4
C_0 (ng/mL)	2615	1750	1900	1580
$t_{1/2}$ (hr)	0.6	0.3	0.1	0.7
Vd_{ss} (L/kg)	0.1	0.3	0.2	0.7
CL (mL/min/kg)	2.8	22.2	24.8	17.8
% LBF	1.9	14.6	16.3	11.7
AUC_{inf} (ng.hr/mL)	2350	300	270	370
AUC_{all} (ng.hr/mL)	2330	300	270	360
Brain PK Parameters (mean):				
Brain concentration (ng/mL) 1 hr 4 hr	<LLOQ <LLOQ	<LLOQ <LLOQ	<LLOQ <LLOQ	<LLOQ <LLOQ

[a] Male C57BL/6J mice; i.v. solution formulation in 10% DMSO/90% HPCD (20% w/v); N = 3 per time point; blood levels measured at 0.08, 0.25 0.5, 1, 2, 4, 8 and 24 hr; terminal brain levels measured at 1 and 4 hr; LOQ, limit of quantification (5-10 ng/mL); <LLOQ, below lower limit of quantification. This study employed the 4 test compounds and a brain penetrant control. All animals appeared normal throughout the duration of the study.

The triazolopyridizinone series **4** presents potent inhibition of Notum in a biochemical assay with IC_{50} values for the most potent analogues comparable to the best compounds described in the literature (<10 nM) such as LP-922056 (**Table 5**).[3,4] These findings are further supported for several representatives from the series by experimentally determined binding modes and their ability to restore Wnt signaling in a cell-based system. As such, this series provide novel and structurally distinct inhibitors of Notum.

We propose that complementary chemotypes will offer an advantage in Notum target validation studies where the properties of the inhibitor should be aligned with the requirements of the disease model. The lack of BBB permeability of **4** may prove to be an advantage for use in peripheral disease models such as bone formation[38] and colorectal cancer.[39]

CONCLUSIONS

A docking-based virtual screen of a large commercial library was used to shortlist 952 compounds for experimental validation as inhibitors of Notum in a biochemical assay. The VS was successful with 44 compounds having an average inhibition >50% at 1 μM (hit rate 4.6%), which narrowed to 31 compounds with an IC_{50} <500 nM. These 31 hits consisted of four clusters of structurally similar compounds along with eight singletons. A critical selection process was then applied to remove PAINs and two clusters (**1**, **2**) and two singletons (**3**, **4d**) were selected for hit validation and expansion.

Cluster **1** was subsequently deselected as representative examples had very low solubility that confounded interpretation of cell-based screens, and the activities of cluster **2** failed to reproduce with resynthesized solid samples. A high-resolution crystal structure of the Notum-**3** complex revealed that a covalent adduct had formed with Ser232 of the catalytic triad. The VS identified ester **3** as a new covalent inhibitor of Notum.

Hit expansion and optimization of preferred singleton **4d** (IC_{50} 27 nM) by SAR of the pendant aryl ring guided by SBDD identified a number of potent inhibitors of Notum activity, e.g. **4f**, **4p** and **4y** (IC_{50} <10 nM). These three inhibitors, along with the original hit **4d**, restored Wnt/β-catenin signaling in a cell-based assay in the presence of Notum. Pilot mouse PK studies were performed and all four examples from this series showed a modest plasma half-life but with negligible brain penetration.

Multiple X-ray structures established the binding of the triazolopyradizinones in Notum. The head-group bound in the entrance to the active site, with the carbonyl oxygen occupying the oxyanion hole,

and the lipophilic aryl ring extending deep into the hydrophobic pocket. Comparison of the original VS binding pose generated by Glide with the X-ray structure for **4d**, revealed a close match with the overall positioning of the compound in close agreement.

In summary, compounds **4d, 4f, 4p** and **4y** are potent inhibitors of Notum carboxylesterase activity that restore Wnt signaling *in vitro* in a cell-based model, although they have limited potential for use *in vivo*. The triazolopyradizinones series **4** represents a new chemical class of Notum inhibitors and the first to be discovered by a VS campaign. These results demonstrate the value of VS with well-designed docking models based on X-ray structures. The discovery of several fragment-sized nanomolar inhibitors of Notum directly out of a VS is noteworthy.[40]

EXPERIMENTAL SECTION

Compound library

Commercially available compounds from ChemDiv (San Diego CA, US) (approximately 1.5 million compounds) were obtained as an sd-file and filtered for molecular properties using ChemAxon[41] cxcalc: MW (200-500); TPSA (20-120); HBD (≤ 2); logD (-4 - 5); NRB (<10); compounds with ring assemblies >13 atoms were also removed. Additional filters removed compounds with a SFI > 7,[42] potentially reactive groups,[43] as well as compounds with an MPO score < 3.5.[44] After filtering, 534,804 compounds were submitted for docking.

Docking

Docking was conducted using Schrödinger Glide SP (version 80012) using FORCEPLANAR True and all other settings at default.[21,22] Prior to docking, the library was prepared using Schrödinger LigPrep 2.4 with default settings to enumerate chiralities, tautomers, and protonation states. Notum structure 6T2K[12] was used for the docking and prepared using the Protein Preparation Wizard. All waters were deleted. Glide

Receptor Grid generation with default settings was used to generate a grid for docking. High scoring hits from the virtual screen were purchased as liquid stock solutions (50 μL at 10 mM in DMSO) for biochemical screening.

Notum OPTS biochemical assay

Methods have been described in detail.[8,10]

Notum TCF/LEF reporter (Luciferase) cell-based assay

Methods used for the TCF/LEF assay for SAR screening of **4a**-**4gg** (**Table 3**) have been described in detail.[8,10] Preferred inhibitors **4d, 4f, 4p** and **4y** were revaluated under slightly modified experimental conditions with a higher concentration of WNT3A (200 ng/mL) (**Table 5**), which gave an improved assay signal window.

Twenty-four hours prior to compound addition, HEK293T cells stably-expressing TCF-LEF were plated at 1×10^4 cells per 20 μL of growth media (DMEM 1× GlutaMax, 4.5 g/L D-glucose, Pyruvate with 10% Fetal Bovine Serum (FBS) and 1% penicillin–streptomycin) in 384-well microplate (Greiner, #781080) and were incubated overnight at 37 °C. An echo liquid handler was used to acoustically dispense 50 nL of compound/DMSO into the V-well polypropylene microplate (Greiner, #781280) to create a 10-point curve. Treatment media (same composition as growth media but FBS reduced to 2.5%), recombinant Notum (500 ng/mL) and recombinant WNT3A (100 ng/mL or 200 ng/mL) (Bio-Techne, #5036-WN-500) were added to the compound plates (in the presence or absence of Notum). The plates were centrifuged (1000 RPM, 1 minute) and incubated for 1 hour at room temperature. The media was removed from the cell plates and 20 μL of treatment media containing the test compounds, Notum and WNT3A from the compound plates were added to cell plates using a Cybio SELMA. The cell plates were incubated at 37 °C for 16-20 hours. For luciferase assay, steady-glo luciferase assay buffer (20 μL, Promega E2520) was

applied to the cell plates, and the luminescence was measured on a PHERAstar FSX microplate reader with an excitation wavelength of 458 nm and an emission wavelength of 520 nm.

Structural Biology

The methods of protein production, crystallization, data collection and structure determination have been described in detail. [10] Data collection and refinement statistics are presented in **Table S2**.

ADME assays

Selected compounds were screened for aqueous solubility, transit performance in MDCK-MDR1 cell lines for permeability, metabolic stability in liver microsomes as a measure of clearance, binding to plasma proteins and acidic dissociation constant (pK_a). Assay protocols and additional data is presented in the Supporting Information (**Tables S1-S8**). ADME studies reported in this work were independently performed by GVK Biosciences (Hyderabad, India) or WuXi AppTec (China).

Mouse pharmacokinetic studies

In vivo mouse pharmacokinetic data was generated at Concept Life Sciences (Chapel-en-le-Frith, U.K.). Assay protocols and additional data is presented in the Supporting Information (**Tables S9-S10, Figure S6**).

Chemistry

General Information.[10] Unless preparative details are provided, all reagents were purchased from commercial suppliers and used without further purification. Solvents were of ACS reagent grade or higher and purchased from commercial suppliers without further purification. Anhydrous solvents were purchased as such from Acros Organics or Sigma-Aldrich. Microwave assisted reactions were performed in a Biotage Initiator+. Thin-layer chromatography (TLC) was carried out on aluminum-backed silica plates. The plates were visualized under UV (254 nm) light, followed by staining with phosphomolybdic acid dip or potassium permanganate and gentle heating. Organic solvent layers were routinely dried with

anhydrous Na_2SO_4 or $MgSO_4$ and concentrated using a Büchi rotary evaporator. Compound purification by column chromatography was performed using a Biotage Isolera using prepacked Biotage SNAP KP-Sil silica cartridges or Biotage SNAP Ultra C18 reverse phase cartridges. ^1H and ^{13}C NMR spectra were recorded in deuterated (≥99.5%) solvents on either a Bruker Avance 300 (300 MHz), Bruker Avance 400 (400 MHz), Bruker Avance 600 (600 MHz), or Bruker Avance 700 (700 MHz). Chemical shifts (δ) are reported as parts per million (ppm), coupling constants (*J*) are reported in Hz, and signal multiplicities are reported as singlet (s), doublet (d), triplet (t), quartet (q), pentet (p), quintet (qu), sextet (sext), doublet of doublets (dd), doublet of triplets (dt), triplet of doublets (td), triplet of triplets (tt), multiplet (m), or broad singlet (br s). Liquid chromatography–mass spectrometry (LCMS) analysis was performed on a Waters Acquity H-Class UPLC system with either an acidic (HSS C18 Column, H_2O/MeCN, 0.1% TFA) or a basic (BEH C18 Column, H_2O/MeCN, 10 mM NH_4OH) mobile phase. The observed mass and isotope pattern matched the corresponding theoretical values as calculated from the expected elemental formula.

The purity of compounds **1-4** was evaluated by NMR spectroscopy and LCMS analysis. All compounds had purity ≥95% unless otherwise stated.

*Preparation of oxazol-5(4H)-ones **1** (General Method 1).*

To a stirred solution of the aldehyde **6** (0.56 mmol) in Ac_2O (2.0 mL) was added NaOAc (46 mg, 0.56 mmol) and the formamidoacetic acid **5** (0.56 mmol). The reaction was heated to 140 °C for 2 h and then allowed to cool to RT. The reaction was quenched with H_2O and the product was extracted with CH_2Cl_2. Solvents were removed in vacuo and exchanged with DMSO. Products **1** were then purified by reverse phase flash silica chromatography (20-100% MeCN:H_2O, 0.1% NH_4OH). Compounds were assigned as Z stereochemistry based on correlation with literature ^1H NMR shift data.[28]

Preparation of [1,3,4]Thiadiazolo[2,3-c][1,2,4]triazin-4-ones **2** *(General Method 2).*

4-Amino-6-methyl-3-sulfanyl-4,5-dihydro-1,2,4-triazin-5-one (**8**) (79 mg, 0.50 mmol) was added to a stirred suspension of the acid **7** (1.0 mmol) in POCl$_3$ (1.0 mL, 11.0 mmol) at RT in a 10 mL microwave vial. The mixture was slowly heated to 90 $^{\circ}$C (external) and stirred for 1 h. The mixture was cooled to RT and poured onto a stirred solution of saturated aqueous NaHCO$_3$ (40 mL). After gas evolution ceased, EtOAc (120 mL) was added. The organic layer was separated, dried, and concentrated under reduced pressure. The product **2** was purified by reverse phase flash silica chromatography (0-100% MeCN:H$_2$O, 0.1% formic acid modifier).

Preparation of [1,2,4]triazolo[4,3-b]pyradizin-3(2H)-ones **4** *(General Method 3).*

A solution of aryl thiol **9** (0.29 mmol), 6-chloro-2H,3H-[1,2,4]triazolo[4,3-b]pyridazin-3-one (**10**) (50 mg, 0.29 mmol) and Cs$_2$CO$_3$ (96 mg, 0.30 mmol) in DMF (1 mL) was heated to 150 $^{\circ}$C under microwave irradiation for 30 min. The products were purified directly by reverse phase flash silica chromatography (0-100% MeCN:H$_2$O, 0.1% formic acid).

Notum inhibitors

*(4Z)-2-(2,4-dichlorophenyl)-4-(2-furylmethylene)oxazol-5-one (**1j**)*

Prepared following General Method 1 with furfural (46 µL, 0.56 mmol) and 2-[(2,4-dichlorophenyl)formamido]acetic acid (139 mg, 0.56 mmol). Product isolated as a brown solid (7 mg, 0.02 mmol, 4%).

^{1}H NMR (600 MHz, CDCl$_3$) δ 8.03 (d, *J* = 8.5 Hz, 1H), 7.72 – 7.57 (m, 3H), 7.40 (d, *J* = 8.5, 1.2 Hz, 1H), 7.26 (m, 1H, under solvent peak), 6.67 (d, *J* = 2.0 Hz, 1H).

13C NMR (151 MHz, CDCl₃) δ 166.36, 160.08, 150.58, 147.34, 139.14, 135.43, 132.54, 132.07, 129.79, 127.68, 122.63, 121.13, 120.22, 114.34.

LCMS (acidic method) R_t 2.08 min, m/z 308.0 [M+H]⁺.

*(4Z)-2-(3,4-dimethylphenyl)-4-[(5-methyl-2-furyl)methylene]oxazol-5-one (**1k**)*

Prepared following General Method 1 with 5-methylfurfural (51 μL, 0.56 mmol) and 2-[(3,4-dimethylphenyl)formamido]acetic acid (120 mg, 0.56 mmol). Product isolated as a yellow solid (50 mg, 0.18 mmol, 32%).

¹H NMR (600 MHz, CDCl3) δ 7.91 (s, 1H), 7.86 (d, J = 7.8 Hz, 1H), 7.48 (s, 1H), 7.26 (s, 1H, under solvent peak), 7.07 (s, 1H), 6.29 (d, J = 3.3 Hz, 1H), 2.44 (s, 3H), 2.34 (d, J = 2.8 Hz, 6H).

¹³C NMR (151 MHz, CDCl3) δ 167.77, 162.67, 158.01, 149.50, 142.91 (signals overlapping), 137.55, 130.37, 129.19, 125.95, 123.31, 122.14, 117.92, 111.05, 20.38, 19.91, 14.41.

LCMS (acidic method) R_t 2.20 min, m/z 282.0 [M+H]⁺.

3-Methyl-7-[(2-methylphenoxy)methyl]-[1,3,4]thiadiazolo[2,3-c][1,2,4]triazin-4-one (**2a**)

Prepared by General Method 2 with **8** (79 mg, 0.50 mmol) and (2-methylphenoxy)acetic acid (170 mg, 1.0 mmol). Product isolated as a pale orange solid. (67 mg, 0.23 mmol, 47%).

¹H NMR (700 MHz, DMSO-*d₆*) δ 7.24 – 7.16 (m, 2H), 7.10 (d, *J* = 7.9 Hz, 1H), 6.94 (td, *J* = 7.4, 0.8 Hz, 1H), 5.58 (s, 2H), 2.43 (s, 3H), 2.24 (s, 3H).

¹³C NMR (176 MHz, DMSO-*d₆*) δ 162.07, 159.24, 155.07, 153.78, 148.58, 130.83, 127.14, 126.08, 121.88, 112.22, 64.69, 17.13, 15.89.

LCMS (acidic method) R_t 1.66 min, m/z 289.1 [M+H]⁺.

7-(3,4-Dimethylphenyl)-3-methyl-[1,3,4]thiadiazolo[2,3-c][1,2,4]triazin-4-one (**2b**)

Prepared by General Method 2 with **8** (79 mg, 0.50 mmol) and 3,4-dimethylbenzoic acid (150 mg, 1.0 mmol). Product isolated as a white solid (12 mg, 0.044 mmol, 8.8%).

^{1}H NMR (700 MHz, DMSO-d_6) δ 7.79 (s, 1H), 7.74 (dd, J = 7.8, 1.9 Hz, 1H), 7.40 (d, J = 7.9 Hz, 1H), 2.44 (s, 3H), 2.34 (s, 3H), 2.33 (s, 3H).

LCMS (acidic method) R$_t$ 1.73 min, m/z 273.1 [M+H]$^+$.

Methyl 4-(indolin-1-yl)-4-oxobutanoate (**3**)

Initially purchased from ChemDiv (San Diego CA, US) (catalogue number 2663-0001). For detailed synthetic methods and characterization data, see reference 31.

6-(Phenylsulfanyl)-2H-[1,2,4]triazolo[4,3-b]pyridazin-3-one (**4a**)

A solution of sodium thiophenolate (50 mg, 0.38 mmol), 6-chloro-2H,3H-[1,2,4]triazolo[4,3-*b*]pyridazin-3-one (**10**) (78 mg, 0.45 mmol) and Cs$_2$CO$_3$ (148 mg, 0.45 mmol) in DMF (1 mL) was heated to 150 °C for 2 h. The product was purified directly by reverse phase flash silica chromatography (0-100% MeCN:H$_2$O, 10 mM NH$_4$OH) to give **4a** (12 mg, 0.05 mmol, 13%) as an off-white solid.

^{1}H NMR (600 MHz, DMSO-d_6) δ 12.71 (s, 1H), 7.68 (d, J = 9.9 Hz, 1H), 7.66 – 7.60 (m, 2H), 7.53 – 7.47 (m, 3H), 6.79 (d, J = 9.9 Hz, 1H).

^{13}C NMR (151 MHz, DMSO-d_6) δ 154.1, 149.5, 137.2, 134.2, 129.9, 129.8, 128.1, 125.2, 122.8.

LCMS (basic method) R$_t$ 1.38 min, m/z 245.0 [M+H]$^+$.

6-(o-Tolylsulfanyl)-2H-[1,2,4]triazolo[4,3-b]pyridazin-3-one (**4b**)

Prepared by General Method 3 with 2-methylbenzenethiol (0.02 mL, 0.15 mmol). Product isolated as a yellow solid (3 mg, 0.012 mmol, 7.9%).

¹H NMR (700 MHz, CDCl₃) δ 10.64 (s, 1H), 7.58 (d, *J* = 7.7 Hz, 1H), 7.39 (t, *J* = 7.4 Hz, 1H), 7.36 (d, *J* = 7.4 Hz, 1H), 7.32 – 7.26 (m, 2H, under solvent peak), 6.52 (d, *J* = 9.9 Hz, 1H), 2.44 (s, 3H).

¹³C NMR (176 MHz, CDCl₃) δ 156.56, 149.96, 142.98, 137.74, 136.55, 131.53, 130.98, 127.48, 127.19, 124.14, 123.08, 21.15.

LCMS (acidic method) R$_t$ 1.39 min, m/z 259.1 [M+H]⁺.

6-(m-Tolylsulfanyl)-2H-[1,2,4]triazolo[4,3-b]pyridazin-3-one (**4c**)

Prepared by General Method 3 with 3-methylbenzenethiol (0.04 mL, 0.30 mmol). Product isolated as a yellow solid (40 mg, 0.15 mmol, 53%).

¹H NMR (600 MHz, DMSO-*d₆*) δ 12.75 (s, 1H), 7.69 (d, *J* = 9.9 Hz, 1H), 7.48 – 7.36 (m, 3H), 7.32 (d, *J* = 7.4 Hz, 1H), 6.80 (d, *J* = 9.9 Hz, 1H), 2.34 (s, 3H).

¹³C NMR (151 MHz, DMSO-*d₆*) δ 154.50, 148.98, 139.53, 137.17, 134.54, 131.34, 130.56, 129.77, 127.73, 125.23, 123.19, 20.78.

LCMS (acidic method) R$_t$ 1.59 min, m/z 259.1 [M+H]⁺.

6-(p-Tolylsulfanyl)-2H-[1,2,4]triazolo[4,3-b]pyridazin-3-one (**4d**)

Prepared by General Method 3 with 4-methylbenzenethiol (0.04 mL, 0.30 mmol. Product isolated as a yellow solid (40 mg, 0.15 mmol, 53%).

¹H NMR (600 MHz, methonal-*d₄*) δ 7.51 (m, 3H), 7.30 (d, *J* = 7.9 Hz, 2H), 6.76 (d, *J* = 9.9 Hz, 1H), 2.39 (s, 3H).

¹³C NMR (151 MHz, methonal-*d₄*) δ 158.39, 151.54, 141.91, 139.17, 136.17, 131.73, 125.56, 125.36, 124.47, 21.31.

LCMS (acidic method) R$_t$ 1.63 min, m/z 259.1 [M+H]⁺ (**Figure S8**).

6-(2-Chlorophenyl)sulfanyl-2H-[1,2,4]triazolo[4,3-b]pyridazin-3-one (**4e**)

Prepared by General Method 3 with 2-chlorobenzenethiol (0.04 mL, 0.29 mmol). Product isolated as a yellow solid (20 mg, 0.72 mmol, 25%).

^{1}H NMR (600 MHz, DMSO-d_6) δ 12.78 (s, 1H), 7.78 – 7.67 (m, 3H), 7.55 (td, J = 7.7, 1.5 Hz, 1H), 7.46 (td, J = 7.7, 1.5 Hz, 1H), 6.93 (d, J = 9.9 Hz, 1H).

^{13}C NMR (151 MHz, DMSO-d_6) δ 152.85, 148.93, 137.15, 137.00, 136.48, 131.85, 130.56, 128.52, 127.27, 125.53, 123.14.

LCMS (acidic method) R_t 1.55 min, m/z 279.0 [M+H]$^+$.

6-(3-Chlorophenyl)sulfanyl-2H-[1,2,4]triazolo[4,3-b]pyridazin-3-one (**4f**)

Prepared by General Method 3 with 3-chlorobenzenethiol (0.04 mL, 0.29 mmol). Product isolated as a yellow solid (43 mg, 0.15 mmol, 53%).

^{1}H NMR (600 MHz, DMSO-d_6) δ 12.76 (s, 1H), 7.75 (t, J = 1.8 Hz, 1H), 7.73 (d, J = 9.9 Hz, 1H), 7.61 – 7.56 (m, 2H), 7.52 (t, J = 7.9 Hz, 1H), 6.93 (d, J = 9.9 Hz, 1H).

^{13}C NMR (151 MHz, DMSO-d_6) δ 153.50, 148.96, 137.22, 133.99, 133.10, 132.51, 131.44, 130.44, 129.70, 125.46, 123.52.

LCMS (acidic method) R_t 1.71 min, m/z 279.1 [M+H]$^+$ (**Figure S9**).

6-(4-Chlorophenyl)sulfanyl-2H-[1,2,4]triazolo[4,3-b]pyridazin-3-one (**4g**)

Prepared by General Method 3 with 4-chlorothiophenol (0.080 mL, 0.56 mmol). Product isolated as an off-white solid (9 mg, 0.032 mmol, 5.7%).

^{1}H NMR (600 MHz, DMSO-d_6) δ 12.75 (s, 1H), 7.71 (d, J = 9.9 Hz, 1H), 7.65 (d, J = 8.6 Hz, 2H), 7.57 (d, J = 8.6 Hz, 2H), 6.91 (d, J = 9.9 Hz, 1H).

^{13}C NMR (151 MHz, DMSO-d_6) δ 153.89, 148.94, 137.21, 135.99, 134.81, 129.86, 126.92, 125.35, 123.29.

LCMS (acidic method) R_t 1.67 min, m/z 279.0 [M+H]$^+$.

6-(2-Fluorophenyl)sulfanyl-2H-[1,2,4]triazolo[4,3-b]pyridazin-3-one (**4h**)

Prepared by General Method 3 with 2-fluorothiophenol (38 mg, 0.29 mmol). Product isolated as a yellow solid (38 mg, 0.15 mmol, 49%).

^{1}H NMR (600 MHz, DMSO-d_6) δ 12.76 (s, 1H), 7.76 – 7.69 (m, 2H), 7.66 – 7.59 (m, 1H), 7.44 (t, J = 8.8 Hz, 1H), 7.38 – 7.32 (m, 1H), 6.98 (d, J = 9.9 Hz, 1H).

^{13}C NMR (151 MHz, DMSO-d_6) δ 161.94 (d, J = 247.6 Hz), 152.92, 148.88, 137.16,136.98 (d, J = 52.6 Hz), 133.21 (d, J = 8.5 Hz), 125.76 (d, J = 3.4 Hz), 125.39, 122.63, 116.59 (d, J = 22.1 Hz), 114.42 (d, J = 18.4 Hz).

LCMS (acidic method) R^t 1.49 min, m/z 263.1 [M+H]$^+$.

6-(3-Fluorophenyl)sulfanyl-2H-[1,2,4]triazolo[4,3-b]pyridazin-3-one (**4i**)

Prepared by General Method 3 with 3-fluorothiophenol (38 mg, 0.29 mmol). Product isolated as a yellow solid (30 mg, 0.11 mmol, 39%).

^{1}H NMR (600 MHz, DMSO-d_6) δ 12.77 (s, 1H), 7.72 (d, J = 9.9 Hz, 1H), 7.58 – 7.51 (m, 2H), 7.48 – 7.43 (m, 1H), 7.39 – 7.32 (m, 1H), 6.92 (d, J = 9.9 Hz, 1H).

^{13}C NMR (151 MHz, DMSO-d_6) δ 162.20 (d, J = 247.4 Hz), 153.45, 148.99, 137.21, 131.60 (d, J = 8.2 Hz), 130.50 (d, J = 8.1 Hz), 129.79 (d, J = 2.4 Hz), 125.46, 123.54, 120.43 (d, J = 23.1 Hz), 116.72 (d, J = 21.1 Hz).

LCMS (acidic method) R_t 1.56 min, m/z 263.0 [M+H]$^+$.

6-(4-Fluorophenyl)sulfanyl-2H-[1,2,4]triazolo[4,3-b]pyridazin-3-one (**4j**)

Prepared by General Method 3 with 4-fluorothiophenol (38 mg, 0.29 mmol). Product isolated as a yellow solid (44 mg, 0.17 mmol, 57%).

^{1}H NMR (600 MHz, DMSO-d_6) δ 12.74 (s, 1H), 7.76 – 7.66 (m, 3H), 7.37 (m, 2H), 6.88 (d, J = 9.9 Hz, 1H).

^{13}C NMR (151 MHz, DMSO-d_6) δ 163.11 (d, J = 248.4 Hz), 154.45, 148.95, 137.22 (d, J = 8.8 Hz), 137.21,

125.21, 123.23 (d, J = 3.2 Hz), 122.94, 117.06 (d, J = 22.1 Hz).

LCMS (acidic method) Rt 1.51 min, m/z 263.1 [M+H]$^+$.

6-[2-(Trifluoromethyl)phenyl]sulfanyl-2H-[1,2,4]triazolo[4,3-b]pyridazin-3-one (**4k**)

Prepared by General Method 3 with 2-(trifluoromethyl)benzenethiol (52 mg, 0.29 mmol). Product isolated

as a yellow solid (24 mg, 0.077 mmol, 26%).

^{1}H NMR (700 MHz, DMSO-d_6) δ 12.75 (s, 1H), 7.95 (dd, J = 7.7, 1.3 Hz, 1H), 7.86 (d, J = 7.7 Hz, 1H), 7.80 –

7.70 (m, 3H), 6.89 (d, J = 9.9 Hz, 1H).

^{13}C NMR (176 MHz, DMSO-d_6) δ 153.57, 148.88, 138.51, 137.10, 133.76, 131.29 (d, J = 29.6 Hz), 130.71,

127.62 (d, J = 5.4 Hz), 126.45, 125.59, 124.40 (d, J = 274.1 Hz), 123.21.

LCMS (acidic method) R$_t$ 1.64 min, m/z 313.0 [M+H]$^+$.

6-[3-(Trifluoromethyl)phenyl]sulfanyl-2H-[1,2,4]triazolo[4,3-b]pyridazin-3-one (**4l**)

Prepared by General Method 3 with 3-(trifluoromethyl)benzenethiol (52 mg, 0.29 mmol). Product isolated

as a yellow solid (20 mg, 0.064 mmol, 22%).

^{1}H NMR (700 MHz, DMSO-d_6) δ 12.73 (s, 1H), 8.00 (s, 1H), 7.92 (dd, J = 7.9, 0.6 Hz, 1H), 7.85 (dd, J = 7.9,

0.6 Hz, 1H), 7.74 – 7.69 (m, 2H), 6.96 (d, J = 9.9 Hz, 1H).

^{13}C NMR (176 MHz, DMSO-d_6) δ 153.28, 148.99, 137.95, 137.23, 130.83, 130.35 (q, J = 32.6 Hz), 130.16 (q,

J = 3.7 Hz), 130.06, 126.34 (q, J = 3.7 Hz), 125.49, 123.67 (q, J = 272.7 Hz), 123.48.

LCMS (acidic method) R$_t$ 1.66 min, m/z 313.0 [M+H]$^+$.

6-[4-(Trifluoromethyl)phenyl]sulfanyl-2H-[1,2,4]triazolo[4,3-b]pyridazin-3-one (**4m**)

Prepared by General Method 3 with 4-(trifluoromethyl)benzenethiol (52 mg, 0.29 mmol). Product isolated as an off-white solid (23 mg, 0.074 mmol, 25%).

^{1}H NMR (700 MHz, DMSO-d_6) δ 12.77 (s, 1H), 7.82 (s, 4H), 7.73 (d, J = 9.8 Hz, 1H), 6.97 (d, J = 9.8 Hz, 1H).

^{13}C NMR (176 MHz, DMSO-d_6) δ 152.77, 148.99, 137.21, 134.48, 133.62, 129.34 (q, J = 32.2 Hz), 126.46 (q, J = 3.6 Hz), 125.68, 123.96 (q, J = 272.3 Hz), 123.95.

LCMS (acidic method) R$_t$ 1.67 min, m/z 313.0 [M+H]$^+$.

6-(3-Methoxyphenyl)sulfanyl-2H-[1,2,4]triazolo[4,3-b]pyridazin-3-one (**4n**)

Prepared by General Method 3 with 3-methoxythiophenol (41 mg, 0.29 mmol). Product isolated as a yellow solid (41 mg, 0.15 mmol, 51%).

^{1}H NMR (600 MHz, DMSO-d_6) δ 12.76 (s, 1H), 7.69 (d, J = 9.9 Hz, 1H), 7.41 (t, J = 8.0 Hz, 1H), 7.23 − 7.15 (m, 2H), 7.07 (ddd, J = 8.4, 2.5, 0.7 Hz, 1H), 6.81 (d, J = 9.9 Hz, 1H), 3.78 (s, 3H).

^{13}C NMR (151 MHz, DMSO-d_6) δ 159.91, 154.24, 149.00, 137.17, 130.81, 129.20, 125.98, 125.25, 123.28, 119.00, 115.73, 55.45.

LCMS (acidic method) R$_t$ 1.57 min, m/z 275.1 [M+H]$^+$.

6-(3-Ethoxyphenyl)sulfanyl-2H-[1,2,4]triazolo[4,3-b]pyridazin-3-one (**4o**)

Prepared by General Method 3 with 3-ethoxythiophenol (45 mg, 0.29 mmol). Product isolated as a yellow solid (58 mg, 0.20 mmol, 69%).

^{1}H NMR (700 MHz, DMSO-d_6) δ 12.72 (s, 1H), 7.67 (d, J = 9.9 Hz, 1H), 7.41 − 7.36 (m, 1H), 7.18 − 7.13 (m, 2H), 7.04 (ddd, J = 8.4, 2.5, 0.9 Hz, 1H), 6.79 (d, J = 9.9 Hz, 1H), 4.04 (q, J = 7.0 Hz, 2H), 1.31 (t, J = 7.0 Hz, 3H).

^{13}C NMR (176 MHz, DMSO-d_6) δ 159.21, 154.26, 149.00, 137.18, 130.81, 129.21, 125.82, 125.24, 123.30, 119.42, 116.16, 63.45, 14.56.

LCMS (acidic method) R$_t$ 1.65 min, m/z 289.1 [M+H]$^+$.

6-[3-(Trifluoromethoxy)phenyl]sulfanyl-2H-[1,2,4]triazolo[4,3-b]pyridazin-3-one (**4p**)

Prepared by General Method 3 with 3-(trifluoromethoxy)thiophenol (57 mg, 0.29 mmol). Product isolated as a yellow solid (46 mg, 0.14 mmol, 48%).

^{1}H NMR (600 MHz, DMSO-*d$_6$*) δ 12.77 (s, 1H), 7.74 (d, *J* = 9.9 Hz, 1H), 7.71 – 7.60 (m, 3H), 7.54 – 7.48 (m, 1H), 6.95 (d, *J* = 9.9 Hz, 1H).

13C NMR (151 MHz, DMSO-*d$_6$*) δ 153.19, 148.95, 148.69, 137.24, 132.67, 131.56, 130.81, 125.99, 125.52, 123.58, 122.15, 120.00 (q, *J* = 257.6 Hz).

LCMS (acidic method) Rt 1.65 min, m/z 328.9 [M+H]$^+$ (**Figure S10**).

6-(3-Isopropoxyphenyl)sulfanyl-2H-[1,2,4]triazolo[4,3-b]pyridazin-3-one (**4q**)

Prepared by General Method 3 with 3-(iso-propoxy)thiophenol (49 mg, 0.29 mmol). Product isolated as a yellow solid (74 mg, 0.25 mmol, 84%).

^{1}H NMR (600 MHz, DMSO-*d$_6$*) δ 12.75 (s, 1H), 7.69 (d, *J* = 9.9 Hz, 1H), 7.38 (t, *J* = 8.1 Hz, 1H), 7.22 – 7.09 (m, 2H), 7.04 (dd, *J* = 8.1, 2.1 Hz, 1H), 6.81 (d, *J* = 9.9 Hz, 1H), 4.66 (hept, *J* = 6.0 Hz, 1H), 1.26 (s, 3H), 1.25 (s, 3H).

^{13}C NMR (151 MHz, DMSO-*d$_6$*) δ 158.15, 154.29, 148.98, 137.18, 130.87, 129.19, 125.63, 125.23, 123.31, 120.44, 117.21, 69.55, 21.73.

LCMS (acidic method) R$_t$ 1.71 min, m/z 303.1 [M+H]$^+$.

6-(3-Methylsulfanylphenyl)sulfanyl-2H-[1,2,4]triazolo[4,3-b]pyridazin-3-one (**4r**)

Prepared by General Method 3 with 3-(methylthio)thiophenol (46 mg, 0.29 mmol). Product isolated as a yellow solid (60 mg, 0.21 mmol, 71%).

¹H NMR (700 MHz, DMSO-d_6) δ 12.72 (s, 1H), 7.69 (d, J = 9.9 Hz, 1H), 7.49 (t, J = 1.7 Hz, 1H), 7.43 − 7.34 (m, 3H), 6.84 (d, J = 9.9 Hz, 1H), 2.49 (s, 3H).

¹³C NMR (176 MHz, DMSO-d_6) δ 154.01, 148.98, 140.39, 137.20, 130.30, 130.14, 130.09, 129.06, 127.00, 125.28, 123.33, 14.49.

LCMS (acidic method) R$_t$ 1.64 min, m/z 291.0 [M+H]⁺.

6-(2,3-Dimethylphenyl)sulfanyl-2H-[1,2,4]triazolo[4,3-b]pyridazine-3-one (**4s**)

Prepared by General Method 3 with 2,3-dimethylthiophenol (41 mg, 0.29 mmol). Product isolated as a yellow solid (34 mg, 0.12 mmol, 43%).

¹H NMR (600 MHz, DMSO-d_6) δ 12.73 (s, 1H), 7.67 (d, J = 9.9 Hz, 1H), 7.46 (d, J = 7.6 Hz, 1H), 7.35 (d, J = 7.6 Hz, 1H), 7.20 (t, J = 7.6 Hz, 1H), 6.74 (d, J = 9.9 Hz, 1H), 2.33 (s, 3H), 2.32 (s, 3H).

¹³C NMR (151 MHz, DMSO-d_6) δ 154.52, 148.97, 140.67, 138.40, 137.16, 133.75, 132.10, 126.97, 126.71, 125.14, 122.65, 20.59, 17.25.

LCMS (acidic method) R$_t$ 1.67 min, m/z 273.1 [M+H]⁺.

6-(2,4-Dimethylphenyl)sulfanyl-2H-[1,2,4]triazolo[4,3-b]pyridazin-3-one (**4t**)

Prepared by General Method 3 with 2,4-dimethylbenzenethiol (0.02mL, 0.15 mmol). Product isolated as a white solid (7 mg, 0.026 mmol, 18%).

¹H NMR (700 MHz, CDCl₃) δ 10.64 (s, 1H), 7.46 (d, J = 7.7 Hz, 1H), 7.37 − 7.24 (m, 1H, under solvent peak), 7.17 (s, 1H), 7.07 (d, J = 7.2 Hz, 1H), 6.51 (d, J = 9.9 Hz, 1H), 2.39 (s, 3H), 2.36 (s, 3H).

¹³C NMR (176 MHz, CDCl₃) δ 157.02, 150.00, 142.87, 141.43, 137.80, 136.65, 132.39, 128.30, 123.99, 123.56, 122.92, 21.41, 21.05.

LCMS (acidic method) R$_t$ 1.49 min, m/z 273.1 [M+H]⁺.

6-(3,4-Dimethylphenyl)sulfanyl-2H-[1,2,4]triazolo[4,3-b]pyridazin-3-one (**4u**)

Prepared by General Method 3 with 3,4-dimethylbenzenethiol (0.02mL, 0.15 mmol). Product isolated as a yellow solid (28 mg, 0.10 mmol, 70%).

^{1}H NMR (700 MHz, CDCl$_3$) δ 7.31 (s, 1H), 7.28 (d, *J* = 7.7 Hz, 1H), 7.23 (d, *J* = 9.8 Hz, 1H), 7.15 (d, *J* = 7.7 Hz, 1H), 6.36 (d, *J* = 9.8 Hz, 1H), 2.25 (s, 3H), 2.23 (s, 3H).

^{13}C NMR (176 MHz, CDCl$_3$) δ 156.03, 152.82, 139.17, 138.71, 137.59, 136.03, 132.64, 131.27, 125.31, 124.23, 121.09, 19.80, 19.74.

LCMS (acidic method) R$_t$ 1.47 min, m/z 273.1 [M+H]$^+$.

6-(3,5-Dimethylphenyl)sulfanyl-2H-[1,2,4]triazolo[4,3-b]pyridazin-3-one (**4v**)

Prepared by General Method 3 with 3,5-dimethylbenzenethiol (0.040 mL, 0.29 mmol). Product isolated as a yellow solid (47 mg, 0.17 mmol, 59%).

^{1}H NMR (700 MHz, DMSO-*d$_6$*) δ 12.71 (s, 1H), 7.66 (d, *J* = 9.9 Hz, 1H), 7.25 – 7.22 (m, 2H), 7.14 – 7.10 (m, 1H), 6.75 (d, *J* = 9.9 Hz, 1H), 2.29 (d, *J* = 0.5 Hz, 6H).

^{13}C NMR (176 MHz, DMSO-*d$_6$*) δ 154.65, 149.00, 139.31, 137.15, 131.70, 131.41, 127.53, 125.20, 123.18, 20.68.

LCMS (acidic method) R$_t$ 1.70 min, m/z 273.1 [M+H]$^+$.

6-(2,3-Dichlorophenyl)sulfanyl-2H-[1,2,4]triazolo[4,3-b]pyridazin-3-one (**4w**)

Prepared by General Method 3 with 2,3-dichlorobenzenethiol (52 mg, 0.29 mmol). Product isolated as an off-white solid (9 mg, 0.029 mmol, 9.8%).

^{1}H NMR (600 MHz, DMSO-*d$_6$*) δ 12.81 (s, 1H), 7.79 (dd, *J* = 8.0 1.4 Hz, 1H), 7.77 (d, *J* = 9.9 Hz, 1H), 7.72 (dd, *J* = 8.0, 1.4 Hz, 1H), 7.46 (t, *J* = 8.0 Hz, 1H), 7.02 (d, *J* = 9.9 Hz, 1H).

^{13}C NMR (151 MHz, DMSO-d_6) δ 152.27, 148.90, 137.15, 134.54, 134.51, 132.93, 131.94, 130.42, 129.16, 125.77, 123.54.

LCMS (acidic method) R$_t$ 2.02 min, m/z 313.0 [M+H]$^+$.

6-(2,4-Dichlorophenyl)sulfanyl-2H-[1,2,4]triazolo[4,3-b]pyridazin-3-one (**4x**)

Prepared by General Method 3 with 2,4-dichlorobenzenethiol (0.040 mL, 0.29 mmol). Product isolated as an off-white solid (40 mg, 0.13 mmol, 44%).

^{1}H NMR (600 MHz, DMSO-d_6) δ 12.79 (s, 1H), 7.91 (d, *J* = 2.3 Hz, 1H), 7.78 (d, *J* = 8.4 Hz, 1H), 7.75 (d, *J* = 9.9 Hz, 1H), 7.56 (dd, *J* = 8.4, 2.3 Hz, 1H), 7.00 (d, *J* = 9.9 Hz, 1H).

^{13}C NMR (151 MHz, DMSO-d_6) δ 152.53, 148.89, 138.21, 137.65, 137.16, 135.78, 130.08, 128.63, 126.44, 125.61, 123.15.

LCMS (acidic method) R$_t$ 1.66 min, m/z 313.0 [M+H]$^+$.

6-(3,4-Dichlorophenyl)sulfanyl-2H-[1,2,4]triazolo[4,3-b]pyridazin-3-one (**4y**)

Prepared by General Method 3 with 3,4-dichlorobenzenethiol (0.040 mL, 0.29 mmol). Product isolated as an off-white solid (25 mg, 0.080 mmol, 27%).

^{1}H NMR (600 MHz, DMSO-d_6) δ 12.76 (s, 1H), 7.97 (d, *J* = 2.1 Hz, 1H), 7.76 (d, *J* = 8.4 Hz, 1H), 7.73 (d, *J* = 9.9 Hz, 1H), 7.62 (dd, *J* = 8.4, 2.1 Hz, 1H), 6.99 (d, *J* = 9.9 Hz, 1H).

^{13}C NMR (151 MHz, DMSO-d_6) δ 153.28, 148.95, 137.25, 135.23, 134.04, 132.69, 132.11, 131.63, 129.06, 125.51, 123.52.

LCMS (acidic method) Rt 1.71 min, m/z 312.9 [M+H]$^+$ (**Figure S11**).

6-(2,3-Difluorophenyl)sulfanyl-2H-[1,2,4]triazolo[4,3-b]pyridazin-3-one (**4z**)

Prepared by General Method 3 with 2,3-difluorobenzenethiol (43 mg, 0.29 mmol). Product isolated as a yellow solid (20 mg, 0.071 mmol, 24%).

^{1}H NMR (600 MHz, DMSO-d_6) δ 12.78 (s, 1H), 7.76 (d, J = 9.9 Hz, 1H), 7.72 – 7.64 (m, 1H), 7.55 (dd, J = 7.7, 6.2 Hz, 1H), 7.40 – 7.33 (m, 1H), 7.07 (d, J = 9.9 Hz, 1H).

^{13}C NMR (176 MHz, DMSO-d_6) δ 152.31,150.76 (dd, J = 16.2, 13.3 Hz),149.35 (dd, J = 15.9, 13.3 Hz), 148.86, 137.15, 131.81 (d, J = 3.0 Hz), 125.86 (dd, J = 7.0, 4.8 Hz), 125.58, 122.72, 120.27 (d, J = 17.2 Hz), 117.02 (d, J = 14.8 Hz).

LCMS (acidic method) R_t 1.52 min, m/z 281.0 [M+H]$^+$.

6-(3,4-Difluorophenyl)sulfanyl-2H-[1,2,4]triazolo[4,3-b]pyridazin-3-one (**4aa**)

Prepared by General Method 3 with 3,4-difluorothiophenol (42 mg, 0.29 mmol). Product isolated as a yellow solid (61 mg, 0.22 mmol, 74%).

^{1}H NMR (700 MHz, DMSO-d_6) δ 12.73 (s, 1H), 7.83 (ddd, J = 9.9, 7.7, 2.2 Hz, 1H), 7.71 (d, J = 9.9 Hz, 1H), 7.58 (dt, J = 10.5, 8.6 Hz, 1H), 7.53 – 7.48 (m, 1H), 6.93 (d, J = 9.9 Hz, 1H).

^{13}C NMR (176 MHz, DMSO-d_6) δ 153.73, 150.79 (dd, J = 169.4, 15.2 Hz), 149.36 (dd, J = 170.3, 15.4 Hz), 148.96, 137.23, 131.77 (dd, J = 6.6, 3.7 Hz), 125.40, 124.74 (dd, J = 6.4, 4.0 Hz), 123.57 (d, J = 17.6 Hz), 123.22, 118.84 (d, J = 16.0 Hz).

6-[(4-Methyl-2-pyridyl)sulfanyl]-2H-[1,2,4]triazolo[4,3-b]pyridazin-3-one (**4bb**)

Prepared by General Method 3 with 4-methyl-2(1*H*)-pyridinethione (37 mg, 0.29 mmol). Product isolated as an off-white solid (30 mg, 0.12 mmol, 40%).

^{1}H NMR (700 MHz, DMSO-d_6) δ 12.80 (s, 1H), 8.35 (dd, J = 5.0, 0.5 Hz, 1H), 7.72 (d, J = 9.8 Hz, 1H), 7.48 (dt, J = 1.4, 0.5 Hz, 1H), 7.18 (ddd, J = 5.0, 1.4, 0.5 Hz, 1H), 7.00 (d, J = 9.8 Hz, 1H), 2.31 (s, 3H).

^{13}C NMR (176 MHz, DMSO-d_6) δ 153.69, 151.66, 149.98, 149.21, 149.06, 137.11, 126.39, 125.70, 125.04, 123.70, 20.37.

LCMS (acidic method) R_t 1.38 min, m/z 260.1 [M+H]$^+$.

6-[(5-Methyl-2-pyridyl)sulfanyl]-2H-[1,2,4]triazolo[4,3-b]pyridazin-3-one (**4cc**)

Prepared by General Method 3 with 5-methylpyridine-2(1*H*)-thione (37 mg, 0.29 mmol). Product isolated as a yellow solid (50 mg, 0.19 mmol, 66%).

^{1}H NMR (700 MHz, DMSO-*d₆*) δ 12.77 (s, 1H), 8.39 – 8.36 (m, 1H), 7.71 (d, *J* = 9.8 Hz, 1H), 7.68 (ddd, *J* = 8.1, 2.4, 0.7 Hz, 1H), 7.58 – 7.54 (m, 1H), 6.96 (d, *J* = 9.8 Hz, 1H), 2.30 (s, 3H).

^{13}C NMR (176 MHz, DMSO-*d₆*) δ 152.32, 150.73, 149.93, 149.02, 138.56, 137.11, 132.72, 125.85, 125.69, 125.04, 17.50.

LCMS (acidic method) R_t 1.35 min, m/z 260.1 [M+H]⁺.

6-[(6-Methyl-2-pyridyl)sulfanyl]-2H-[1,2,4]triazolo[4,3-b]pyridazin-3-one (**4dd**)

Prepared by General Method 3 with 2-mercapto-6-methylpyridine (37 mg, 0.29 mmol). Product isolated as a yellow solid (20 mg, 0.077 mmol, 26%).

^{1}H NMR (600 MHz, DMSO-*d₆*) δ 12.82 (s, 1H), 7.75 (d, *J* = 9.9 Hz, 1H), 7.72 (d, *J* = 7.7 Hz, 1H), 7.43 (d, *J* = 7.7 Hz, 1H), 7.23 (d, *J* = 7.7 Hz, 1H), 7.03 (d, *J* = 9.9 Hz, 1H), 2.43 (s, 3H).

^{13}C NMR (151 MHz, DMSO-*d₆*) δ 159.22, 152.87, 151.88, 149.05, 138.29, 137.12, 126.04, 125.05, 122.51, 122.16, 23.84.

LCMS (acidic method) R_t 1.36 min, m/z 260.1 [M+H]⁺.

6-[[6-(Trifluoromethyl)-2-pyridyl]sulfanyl]-2H-[1,2,4]triazolo[4,3-b]pyridazin-3-one (**4ee**)

Prepared by General Method 3 with 2-sulphanyl-6-(trifluoromethyl)pyridine (53 mg, 0.29 mmol). Product isolated as a yellow solid (3 mg, 0.0096 mmol, 3.3%).

^{1}H NMR (700 MHz, DMSO-*d₆*) δ 12.85 (s, 1H), 8.10 (t, *J* = 8.0 Hz, 1H), 7.93 (d, *J* = 8.0 Hz, 1H), 7.84 (d, *J* = 8.0 Hz, 1H), 7.80 (d, *J* = 9.8 Hz, 1H), 7.15 (d, *J* = 9.8 Hz, 1H).

LCMS (acidic method) R_t 1.56 min, m/z 314.0 [M+H]$^+$.

6-Pyrimidin-2-ylsulfanyl-2H-[1,2,4]triazolo[4,3-b]pyridazin-3-one (**4ff**)

Prepared by General Method 3 with 2-mercaptopyrimidine (66 mg, 0.59 mmol). Product isolated as a yellow solid (35 mg, 0.14 mmol, 24%).

^{1}H NMR (700 MHz, DMSO-d_6) δ 8.70 (d, *J* = 4.9 Hz, 2H), 8.25 (s, 1H), 7.81 (d, *J* = 9.8 Hz, 1H), 7.38 (t, *J* = 4.9 Hz, 1H), 7.31 (d, *J* = 9.8 Hz, 1H).

^{13}C NMR (151 MHz, DMSO-d_6) δ 181.42, 168.51, 158.73, 149.53, 149.03, 136.98, 128.63, 124.81, 119.12.

LCMS (acidic method) R_t 1.25 min, m/z 247.1 [M+H]$^+$.

6-Pyrimidin-4-ylsulfanyl-2H-[1,2,4]triazolo[4,3-b]pyridazin-3-one (**4gg**)

Prepared by General Method 3 with 2-mercaptopyrazine (66 mg, 0.59 mmol). Product isolated as a yellow solid (40 mg, 0.16 mmol, 28%).

^{1}H NMR (700 MHz, DMSO-d_6) δ 8.90 (d, *J* = 1.1 Hz, 1H), 8.60 (m, 2H), 8.42 (s, 1H), 7.77 (d, *J* = 9.8 Hz, 1H), 7.12 (d, *J* = 9.8 Hz, 1H).

^{13}C NMR (151 MHz, DMSO-d_6) δ 151.61, 150.72, 149.12, 146.24, 145.10, 143.16, 137.07, 125.74, 125.53.

LCMS (acidic method) R_t 0.95 min, m/z 247.1 [M+H]$^+$.

6-(p-Tolylsulfonyl)-2H-[1,2,4]triazolo[4,3-b]pyridazin-3-one (**4hh**) *and* *6-(p-tolylsulfinyl)-2H-[1,2,4]triazolo[4,3-b]pyridazin-3-one* (**4ii**)

To a solution of 6-(*p*-tolylsulfanyl)-2*H*-[1,2,4]triazolo[4,3-b]pyridazin-3-one (**4d**) (85 mg, 0.33 mmol) in DMF (1.5 mL) at 0 °C was added OXONE® monopersulfate (0.20 g, 1.3 mmol), and the reaction mixture was stirred at RT overnight. A formic acid (ca. 0.50 mL) was added to quench the excess OXONE. DMSO (1.5 mL) was added and solvents were removed *in vacuo*. The product was then purified by reverse phase

flash silica chromatography (15-85% MeCN:H_2O, 0.1% formic acid) and to give **4ii** (first elution peak) and

4hh (second elution peak). Peaks were assigned based on mass ion seen in LCMS analysis.

For **4hh**: dark yellow solid (30 mg, 0.10 mmol, 31%). ^{1}H NMR (600 MHz, DMSO-d_6) δ 13.09 (s, 1H), 8.02 (d,

J = 10.0 Hz, 1H), 7.93 (d, *J* = 8.4 Hz, 2H), 7.54 (dd, *J* = 12.5, 9.0 Hz, 3H), 2.42 (s, 3H).

^{13}C NMR (151 MHz, DMSO-d_6) δ 154.21, 148.91, 146.29, 137.14, 134.09, 130.55, 128.84, 118.60, 21.24

(one tertiary carbon not shown).

 LCMS (acidic method) R$_t$ 1.58 min, m/z 291.0 [M+H]$^+$.

For **4ii**: light yellow solid (42 mg, 0.15 mmol, 47%). ^{1}H NMR (600 MHz, DMSO-d_6) δ 13.01 (s, 1H), 7.93 (d,

J = 9.9 Hz, 1H), 7.67 (d, *J* = 8.2 Hz, 2H), 7.43 (d, *J* = 8.1 Hz, 2H), 7.28 (d, *J* = 9.9 Hz, 1H), 2.36 (s, 3H).

^{13}C NMR (151 MHz, DMSO-d_6) δ 160.87, 149.02, 142.57, 138.85, 137.53, 130.53, 128.41, 124.72, 116.41,

20.96.

 LCMS (acidic method) R$_t$ 1.47 min, m/z 275.1 [M+H]$^+$.

6-(p-Tolylmethyl)-2H-[1,2,4]triazolo[4,3-b]pyridazin-3-one (**4jj**)

2-(Methoxymethyl)-6-(*p*-tolylmethyl)-[1,2,4]triazolo[4,3-*b*]pyridazin-3-one (**12**) (70 mg, 0.24 mmol) was

added to TFA (2.0 mL, 26 mmol) and heated to 55 °C for 18 h. The reaction was cooled to RT, the solvents

evaporated in vacuo and residue dissolved in DMSO (1.5 mL). The product was purified by reverse phase

flash silica chromatography as the DMSO solution was loaded by direct injection onto 30g C18 Si flash

cartridge with gradient elution of 0-100% MeCN:H_2O (0.1% formic acid modifier). Product **4jj** was isolated

as an off white solid (33 mg, 0.14 mmol, 58% yield).

^{1}H NMR (600 MHz, DMSO-d_6) (rotamers) δ 7.70 (d, *J* = 9.8 Hz, 1H), 7.19 (d, *J* = 8.0 Hz, 2H), 7.14 (d, *J* = 7.9

Hz, 2H), 6.97 (d, *J* = 9.8 Hz, 1H), 3.97 (s, 2H), 2.26 (s, 3H).

^{13}C NMR (151 MHz, DMSO-d_6) (rotamers) δ 155.15, 154.80, 149.57, 147.78, 137.68, 136.61, 136.12,

136.08, 133.87, 133.75, 129.38, 129.36, 128.99, 125.22, 125.04, 124.85, 124.33, 68.20, 20.66.

LCMS (acidic method) R_t 1.52 min, m/z 241.1 [M+H]$^+$.

6-(4-Methylanilino)-2H-[1,2,4]triazolo[4,3-b]pyridazin-3-one (**4kk**)

p-TsOH.H$_2$O (130 mg, 0.70 mmol), *p*-toluidine (0.080mL, 0.70 mmol) and 6-chloro-2*H*,3*H*-[1,2,4]triazolo[4,3-*b*]pyridazin-3-one (**10**) (100 mg, 0.59 mmol) were added to a thick-walled reaction vial followed by *n*-BuOH (8 mL). The mixture was stirred rapidly for 5 min at RT, the vial was sealed with a Teflon-lined crimp cap and the reaction was heated to 180 °C under microwave irradiation for 16 h. DMSO (1.5 mL) was added and the volatile solvents were evaporated *in vacuo* to give the reaction mixture as a solution in DMSO. Direct purification by reverse phase flash silica chromatography on 30g C18 Si cartridge with gradient elution of 15-85% MeCN:H$_2$O (0.1% formic acid modifier) gave **4kk** (21 mg, 0.087 mmol, 15%) as a light brown solid.

^{1}H NMR (600 MHz, DMSO-d_6) δ 9.40 (s, 1H), 7.66 (d, *J* = 8.5 Hz, 2H), 7.61 (d, *J* = 9.9 Hz, 1H), 7.15 (d, *J* = 8.2 Hz, 2H), 6.89 (d, *J* = 9.9 Hz, 1H), 2.27 (s, 3H).

LCMS (acidic method) R_t 1.51 min, m/z 242.1 [M+H]$^+$.

6-(N,4-Dimethylanilino)-2H-[1,2,4]triazolo[4,3-b]pyridazin-3-one (**4ll**)

p-TsOH.H$_2$O (100 mg, 0.53 mmol) and 6-chloro-2*H*,3*H*-[1,2,4]triazolo[4,3-*b*]pyridazin-3-one (**10**) (75 mg, 0.44 mmol) were added to a thick-walled reaction vial, and the vial was sealed with a Teflon-lined crimp cap. *n*-BuOH (5 mL) and *N*-methyl-*p*-toluidine (0.07 mL, 0.53 mmol) were added, and the mixture was heated at 180 °C under microwave irradiation for 12h. Formic acid (0.5 mL) and then DMSO (1.5 mL) were added, and volatile solvents were evaporated *in vacuo*. Direct purification by reverse phase flash silica chromatography on 30g C18 Si cartridge with gradient elution of 15-80% MeCN:H$_2$O (0.1% formic acid modifier) gave **4ll** (31 mg, 0.12 mmol, 37%) as an off-white solid.

^{1}H NMR (700 MHz, DMSO-d_6) δ 12.42 (s, 1H), 7.43 (d, J = 10.2 Hz, 1H), 7.28 – 7.23 (m, 2H), 7.20 – 7.16 (m, 2H), 6.48 (d, J = 10.2 Hz, 1H), 3.29 (s, 3H), 2.32 (s, 3H).

LCMS (acidic method) R_t 1.64 min, m/z 256.1 [M+H]$^+$.

6-(4-Methylphenoxy)-2H-[1,2,4]triazolo[4,3-b]pyridazin-3-one (**4mm**)

Prepared by General Method 3 with *p*-cresol (16 mg, 0.15 mmol). Product isolated as an off-white solid (13 mg, 0.054 mmol, 36%).

^{1}H NMR (700 MHz, CDCl$_3$) δ 7.52 (d, J = 9.9 Hz, 1H), 7.20 (d, J = 8.3 Hz, 2H), 7.14 – 7.08 (m, 2H), 6.88 (d, J = 9.9 Hz, 1H), 2.36 (s, 3H).

LCMS (basic method) R_t 1.42 min, m/z 243.2 [M+H]$^+$.

8-Methyl-6-(p-tolylsulfanyl)-2H-[1,2,4]triazolo[4,3-b]pyridazin-3-one (**4nn**)

Prepared by the same two-step method as used for **4oo** but starting from 3,6-dichloro-4-methylpyridazine (**13a**) (0.50 g, 3.1 mmol) to give 6-chloro-8-dimethyl-2*H*-[1,2,4]triazolo[4,3-*b*]pyridazin-3-one (**14a**) as a yellow solid (260 mg, 0.14 mmol, 46%), which was used without further purification. ^{1}H NMR (700 MHz, DMSO-d_6) of the methyl signals showed this to be predominantly the 8-Me isomer (δ 12.86 (s, 1H), 7.13 (q, J = 1.3 Hz, 1H), 2.31 (d, J = 1.4 Hz, 3H)) along with a small amount of the 7-Me isomer (δ 12.86 (s, 1H), 7.78 (q, J = 1.3 Hz, 1H), 2.26 (d, J = 1.4 Hz, 3H)) as a ratio 8-Me:7-Me, 5:1.

Compound **4nn** was then prepared by General Method 3 with 4-methylbenzenethiol (36 mg, 0.29 mmol), 6-chloro-8-methyl-2*H*-[1,2,4]triazolo[4,3-*b*]pyridazin-3-one (**14a**) (54 mg, 0.29 mmol) and Cs$_2$CO$_3$ (95 mg, 0.29 mmol). Product isolated as a yellow solid (37 mg, 0.14 mmol, 46%) as an inseparable mixture of predominantly the 8-Me isomer along with a small amount of the 7-Me isomer as a ratio 8-Me:7-Me, 5:1 by ^{1}H NMR analysis.

8-Methyl isomer (**4nn**): ^{1}H NMR (700 MHz, DMSO-d_6) δ 12.66 (s, 1H), 7.48 (d, J = 8.0 Hz, 2H), 7.32 – 7.27 (m, 2H), 6.71 (q, J = 1.3 Hz, 1H), 2.35 (s, 3H), 2.22 (d, J = 1.4 Hz, 3H).

7-Methyl isomer: ^{1}H NMR (700 MHz, DMSO-d_6) δ 12.48 (s, 1H), 7.57 (q, J = 8.0 Hz, 1H), 7.46 (d, J = 8.0 Hz, 2H), 7.30 – 7.26 (m, 2H), 2.35 (s, 3H), 2.25 (d, J = 1.4 Hz, 3H).

Mixture of 8- and 7-methyl isomers: ^{13}C NMR (176 MHz, DMSO-d_6) δ 155.43, 154.43, 149.27, 148.81, 139.67, 139.50, 138.52, 138.08, 136.10, 134.55, 134.33, 132.64, 130.53, 130.30, 124.46, 123.62, 122.00, 120.71, 48.63, 30.73, 20.89, 20.87, 18.10, 14.39.

LCMS (acidic method) R_t 1.68 min as a single peak, m/z 273.1 [M+H]$^+$.

7,8-Dimethyl-6-(p-tolylsulfanyl)-2H-[1,2,4]triazolo[4,3-b]pyridazin-3-one (**4oo**)

Prepared by General Method 3 with 4-methylbenzenethiol (56 mg, 0.45 mmol), 6-chloro-7,8-dimethyl-2*H*-[1,2,4]triazolo[4,3-*b*]pyridazin-3-one (**14b**) (90 mg, 0.45 mmol) and Cs$_2$CO$_3$ (140 mg, 0.45 mmol). Product isolated as a light yellow solid (99 mg, 0.35 mmol, 76%).

^{1}H NMR (600 MHz, DMSO-d_6) δ 12.53 (s, 1H), 7.47 – 7.42 (m, 2H), 7.29 (d, J = 7.9 Hz, 2H), 2.36 (s, 3H), 2.26 (d, J = 0.8 Hz, 3H), 2.21 (d, J = 0.7 Hz, 3H).

^{13}C NMR (151 MHz, DMSO-d_6) δ 155.40, 149.23, 139.33, 139.09, 134.50, 131.11, 130.27, 128.19, 124.19, 20.89, 14.05, 11.45.

LCMS (acidic method) R_t 1.76 min, m/z 287.1 [M+H]$^+$.

2-Methyl-6-(p-tolylsulfanyl)-[1,2,4]triazolo[4,3-b]pyridazin-3-one (**4pp**)

Prepared by General Method 3 with 4-methylbenzenethiol (56 mg, 0.47 mmol), 6-chloro-2-methyl-2*H*,3*H*-[1,2,4]triazolo[4,3-*b*]pyridazin-3-one (86 mg, 0.47 mmol) and Cs$_2$CO$_3$ (140 mg, 0.47 mmol). Product isolated as an off-white solid (66 mg, 0.24 mmol, 52%).

^{1}H NMR (700 MHz, CDCl$_3$) δ 7.46 (d, *J* = 8.0 Hz, 2H), 7.24 (m, 3H), 6.54 (d, *J* = 9.9 Hz, 1H), 3.67 (s, 3H), 2.39 (s, 3H).

^{13}C NMR (176 MHz, CDCl$_3$) δ 156.86, 148.42, 140.67, 135.75, 135.12, 130.86, 124.78, 123.38, 122.95, 33.63, 21.47.

LCMS (acidic method) R$_t$ 1.70 min, m/z 273.1 [M+H]$^+$.

6-Chloro-2-(methoxymethyl)-[1,2,4]triazolo[4,3-b]pyridazin-3-one (**11**)

6-Chloro-2*H*,3*H*-[1,2,4]triazolo[4,3-*b*]pyridazin-3-one (**10**) (650 mg, 3.8 mmol) was suspended in a mixture of DMF (10 mL) and NEt$_3$ (2.1 mL, 15 mmol), and cooled to 0 °C. Chloromethyl methyl ether (0.58 mL, 7.6 mmol) was added dropwise and stirred over 72 h at RT. The mixture was concentrated to dryness and the residue was dissolved EtOAc (150 ml), washed with water (~100 mL) and then separated. The aqueous phase was washed with EtOAc (2 x 50 mL), and the combined organics washed with sat. brine (20 mL), dried and evaporated. Purified by flash silica chromatography on 50g Si column eluting with 15-100% EtOAc in cyclohexane gave **11** (600 mg, 2.8 mmol, 73%) as a faint yellow solid.

^{1}H NMR (600 MHz, CDCl$_3$) δ 7.49 (dd, *J* = 9.8, 0.5 Hz, 1H), 6.94 (dd, *J* = 9.8, 0.5 Hz, 1H), 5.35 (s, 2H), 3.45 (s, 3H).

^{13}C NMR (151 MHz, CDCl$_3$) δ 148.42, 147.99, 136.45, 126.53, 125.97, 57.60.

LCMS (acidic method) R$_t$ 0.65 min, m/z 215.0 [M+H]$^+$.

2-(Methoxymethyl)-6-(p-tolylmethyl)-[1,2,4]triazolo[4,3-b]pyridazin-3-one (**12**)

2-Dicyclohexylphosphino-2',4',6'-triisopropylbiphenyl (XPhos) (66 mg, 0.14 mmol), palladium acetate (16 mg, 0.070 mmol), and 6-chloro-2-(methoxymethyl)-[1,2,4]triazolo[4,3-*b*]pyridazin-3-one (**11**) (150 mg, 0.70 mmol) were added to an oven dried 2.5 mL thick-walled reaction vial, and the vial was sealed with a Teflon-lined crimp cap. The vial was evacuated and back filled with Ar (x3). THF (5 mL) was added to the

vial with stirring and the mixture stirred for an additional 5 min to solubilise the solids. A solution of 4-methylbenzylzinc chloride (0.5 M in THF) (2.8 mL, 1.4 mmol) was added and the reaction was heated to 65 °C overnight. The mixture was cooled to RT, quenched into sat. aqueous NH$_4$Cl (ca. 50 mL), diluted with EtOAc (100 mL) and the organics were separated. The aqueous phase was washed with EtOAc (2 x 50 mL) and the combined organics were washed with brine, dried and evaporated *in vacuo* to give a brown oil. Purification by reverse phase flash silica chromatography on 30g C18 eluting with 15-85% MeCN:H$_2$O (0.1% formic acid) gave a light brown oil. This was further purified by flash silica chromatography on 12g Si eluting with 0-40% EtOAc in CH$_2$Cl$_2$ to give **12** (77 mg, 0.27 mmol, 39%) as faint yellow oil that crystallized on standing.

^{1}H NMR (600 MHz, DMSO-d_6) δ 7.73 (d, *J* = 9.8 Hz, 1H), 7.20 (d, *J* = 8.0 Hz, 2H), 7.14 (d, *J* = 7.9 Hz, 2H), 7.03 (d, *J* = 9.8 Hz, 1H), 5.21 (s, 2H), 3.98 (s, 2H), 3.30 (s, 3H), 2.27 (s, 3H).

^{13}C NMR (151 MHz, DMSO-d_6) δ 155.20, 148.56, 137.13, 136.13, 133.71, 129.37, 129.02, 125.37, 124.85, 76.08, 56.46, 40.16, 20.66.

LCMS (acidic method) R$_t$ 1.65 min, m/z 285.1 [M+H]$^+$.

6-Chloro-7,8-dimethyl-2H-[1,2,4]triazolo[4,3-b]pyridazin-3-one (**14b**)

To a solution of 3,6-dichloro-4,5-dimethylpyridazine (**13b**) (0.50 g, 3.1 mmol) in EtOH (10 mL) in a thick-walled reaction vial was added semicarbazide hydrochloride (680 mg, 6.1 mmol), H$_2$O (2 mL) and conc. HCl (0.020 mL, 0.25 mmol). The vial was sealed with a Teflon-lined crimp cap and was heated to 85 °C for 72 h. The volatile solvents was evaporated, H$_2$O (5 mL) was added and the mixture neutralized to pH ca. 7 with 2 M NaOH. The solid was collected by filtration, washed with water (5 mL) then Et$_2$O (5 mL), and dried on the filter paper for 2 h to give **14b** (210 mg, 1.0 mmol, 37%) as an off-white solid, which was used without further purification.

^{1}H NMR (600 MHz, DMSO-d_6) δ 12.77 (s, 1H), 2.30 (d, *J* = 0.8 Hz, 3H), 2.23 (d, *J* = 0.8 Hz, 3H).

^{13}C NMR (151 MHz, DMSO-d_6) δ 149.26, 149.00, 138.90, 134.13, 128.57, 15.34, 12.18.

LCMS (acidic method) R_t 1.25 min, m/z 199.0 [M+H]$^+$.

ASSOCIATED CONTENT

Supporting Information

The Supporting Information is available free of charge at …

Scatter plot of virtual screen single point screening results. Chemical structures of VS hits. Residue numbers for human Notum active site. Docking poses of E- and Z-oxazolones. Correlation plot of Notum TCF/LEF vs OPTS screening data. ADME protocols and data. Mouse Pharmacokinetic studies. Data for additional oxazolones. X-ray structure determination: data collection and refinement statistics. Notum pocket electrostatics. Ligand electron-density maps. Supplementary Experimental Section. LCMS traces. Notum OPTS and TCF/LEF screening data curves. (PDF).

Notum docking model (PDB).

Docked poses for all selected compounds with screening data (SDF).

Molecular formula strings and Notum IC$_{50}$ data for **1-4** (CSV).

Screening data set (SMILES, docking scores, % inhib. @ 1 μM (n = 2), % inhib. @ 10 μM (n = 2)) (CSV).

Accession Codes

Coordinates for X-ray structures of Notum crystallized with **4c** (7B3X), **4d** (7B4X), **4e** (7B3G), **4f** (7B3I), **4g** (7B3P), **4p** (7B3H) and **4r** (7B45), **4y** (7B50) have been deposited in the Protein Data Bank. Authors will release the atomic coordinates upon article publication.

AUTHOR INFORMATION
Corresponding Authors

Paul V. Fish - Phone: +44 (0)20 7679 6971; Email: p.fish@ucl.ac.uk; orcid.org/0000-0002-2117-2173.

Fredrik Svensson - Phone: +44 (0)20 7679 0811; Email: f.svensson@ucl.ac.uk; orcid.org/0000-0002-5556-8133

Authors

David Steadman - E-mail: david.steadman.09@ucl.ac.uk; orcid.org/0000-0003-4271-5525

Benjamin N. Atkinson - E-mail: ben.atkinson@ucl.ac.uk.; orcid.org/0000-0001-5511-9859.

Yuguang Zhao - E-mail: yuguang@strubi.ox.ac.uk; orcid.org/0000-0001-8916-8552.

Nicky J. Willis - E-mail: n.willis@ucl.ac.uk; orcid.org/0000-0003-3245-5280.

Sarah Frew - E-mail: sfrew@bioascent.com.

Amy Monaghan - E-mail: amy.monaghan@msd.com.

Chandni Patel - E-mail: c.patel@ucl.ac.uk

Emma Armstrong - E-mail: e.armstrong@ucl.ac.uk

Kathryn Costelloe - E-mail: k.costelloe@ucl.ac.uk

Lorenza Magno - E-mail: l.magno@ucl.ac.uk

Magda Bictash - E-mail: magda.bictash@evotec.com

E. Yvonne Jones - E-mail: yvonne@strubi.ox.ac.uk; orcid.org/0000-0002-3834-1893.

Author contributions

The research was performed through contributions of all authors. D.S., P.V.F. and F.S. wrote the manuscript with additional contributions from Y.Z. All authors have given approval to the final version of the manuscript.

ABBREVIATIONS

ADME, absorption distribution metabolism elimination; BBB, blood-brain barrier; BCRP, breast cancer resistance protein; CNS, central nervous system; DMF, *N,N*-dimethylformamide; DMSO, dimethylsulfoxide; ER, efflux ratio; HAC, heavy atom count; HTS, high throughput screen; LE, ligand efficiency; LLE, lipophilic ligand efficiency; MLM, mouse liver microsomes; MPO, multiparameter

optimization; MRP, multidrug resistance-associated protein; NRB, number of rotatable bonds; OPTS, trisodium 8-octanoyloxypyrene-1,3,6-trisulfonate; PDB, Protein Data Bank; P-gp, P-glycoprotein; PK, pharmacokinetic; RT, room temperature; SAR, structure activity relationship; SBDD, structure-based drug design; SFI, solubility forecast index; THF, tetrahydrofuran; TPSA, topological polar surface area, VS, virtual screening.

REFERENCES AND NOTES

1. Kakugawa, S.; Langton, P. F.; Zebisch, M.; Howell, S. A.; Chang, T. H.; Liu, Y.; Feizi, T.; Bineva, G.; O'Reilly, N.; Snijders, A. P.; Jones, E. Y.; Vincent, J. P. Notum deacylates Wnt proteins to suppress signalling activity. *Nature* **2015**, *519*, 187–192.

2. Zhang, X.; Cheong, S.M.; Amado, N.G.; Reis, A.H.; MacDonald, B.T.; Zebisch, M.; Jones, E.Y.; Abreu, J.G.; He, X. NOTUM is required for neural and head induction via Wnt deacylation, oxidation, and inactivation. *Dev. Cell* **2015**, *32***,** 719–730.

3. Bayle, E. D.; Svensson, F.; Atkinson, B. N.; Steadman, D.; Willis, N. J.; Woodward, H. L.; Whiting, P.; Vincent, J.-P.; Fish, P. V. Carboxylesterase Notum is a druggable target to modulate Wnt signalling. *J. Med. Chem.* **2021**, *64*, 4289–4311

4. Zhao, Y.; Jolly, S.; Benvegnu, S.; Jones, E. Y.; Fish, P. V. Small molecule inhibitors of carboxylesterase Notum. *Fut. Med. Chem.* **2021**, *13*, 1001-1015.

5. Han, Q.; Pabba, P. K.; Barbosa, J.; Mabon, R.; Healy, J. P.; Gardyan, M. W.; Terranova, K. M.; Brommage, R.; Thompson, A. Y.; Schmidt, J. M.; Wilson, A. G. E.; Xu, X.; Tarver, J. E.; Carson, K. G. 4H-Thieno[3,2-c]chromene based inhibitors of Notum pectinacetylesterase. *Bioorg. Med. Chem. Lett.* **2016**, *26*, 1184–1187.

6. Tarver, J. E.; Pabba, P. K.; Barbosa, J.; Han, Q.; Gardyan, M. W.; Brommage, R.; Thompson, A. Y.; Schmidt, J. M.; Wilson, A. G. E.; He, W.; Lombardo, V. K.; Carson, K. G. Stimulation of cortical bone formation with thienopyrimidine based inhibitors of Notum pectinacetylesterase. *Bioorg. Med. Chem. Lett.* **2016**, *26*, 1525–1528.

7. Suciu, R. M.; Cognetta, A. B.; Potter, Z. E.; Cravatt, B. F. Selective irreversible inhibitors of the Wnt deacylating enzyme NOTUM developed by activity-based protein profiling. *ACS Med. Chem. Lett.* **2018**, *9*, 563–568.

8. Atkinson, B. N.; Steadman, D.; Zhao, Y.; Sipthorp, J.; Vecchia, L.; Ruza, R. R.; Jeganathan, F.; Lines, G.; Frew, S.; Monaghan, A.; Kjær, S.; Bictash, M.; Jones, E. Y.; Fish, P. V. Discovery of 2-phenoxyacetamides as inhibitors of the Wnt-depalmitoleating enzyme NOTUM from an X-Ray fragment screen. *Med. Chem. Comm* **2019**, *10*, 1361–1369.

9. Zhao, Y.; Ren, J.; Hillier, J.; Jones, M.; Lu, W.; Jones, E. Y. Structural characterization of melatonin as an inhibitor of the Wnt deacylase Notum. *J. Pineal Res.* **2020**, *68*, e12630.

10. Mahy, W.; Willis, N. J.; Zhao, Y.; Woodward, H. L.; Svensson, F.; Sipthorp, J.; Vecchia, L.; Ruza, R. R.; Hillier, J.; Kjær, S.; Frew, S.; Monaghan, A.; Bictash, M.; Salinas, P. C.; Whiting, P.; Vincent, J. P.; Jones, E. Y.; Fish, P. V. 5-Phenyl-1,3,4-Oxadiazol-2(3H)-Ones are potent inhibitors of Notum carboxylesterase activity identified by the optimization of a crystallographic fragment screening hit. *J. Med. Chem.* **2020**, *63*, 12942–12956.

11. Mahy, W.; Patel, M.; Steadman, D.; Woodward, H.; Atkinson, B. N.; Svensson, F.; Willis, N.; Flint, A.; Papatheodorou, D.; Zhao, Y.; Vecchia, L.; Ruza, R. R.; Hillier, J.; Frew, S.; Monaghan, A.; Costa, A.; Bictash, M.; Walter, M.; Jones, E. Y.; Fish, P. V. Screening of a custom-designed acid fragment library identifies 1-phenylpyrroles and 1-phenylpyrrolidines as inhibitors of Notum carboxylesterase activity. *J. Med. Chem.* **2020**, *63*, 9464–9483.

12. Atkinson, B. N.; Steadman, D.; Mahy, W.; Zhao, Y.; Sipthorp, J.; Bayle, E. D.; Svensson, F.; Papageorgiou, G.; Jeganathan, F.; Frew, S.; Monaghan, A.; Bictash, M.; Yvonne Jones, E.; Fish, P. V. Scaffold-hopping identifies furano[2,3-d]pyrimidine amides as potent Notum inhibitors. *Bioorg. Med. Chem. Lett.* **2019**, 126751.

13. Zhao, Y.; Schuhmacher, L.-N.; Roberts, M.; Hillier, J.; Kagugawa, S.; Bineva-Todd, G.; Howell, S.; O'Reilly, N.; Perret, C.; Snijders, A. P.; Vincent, J.-P.; Jones, E. Y. Notum deacylates octanoylated ghrelin. *Mol. Met.* **2021**, *49*, 101201. doi.org/10.1016/j.molmet.2021.101201

14. There are currently 46 structures available in the PDB under the search term 'Notum', see: https://www.rcsb.org/ (accessed Oct 6, 2021).

15.   Zhao, Y.; Ren, J.; Hillier, J.; Lu, W.; Jones, E. Y. Caffeine inhibits Notum activity by binding at the catalytic pocket. *Commun. Biol.* **2020**, *3*, 555.

16.   Hopkins, A. L.; Groom, C. R. The druggable genome. *Nat. Rev. Drug Discov.* **2002**, *1*, 727–730.

17.   As assessed by Schrödinger SiteMap, which is used to detect and score binding sites. The score is constructed and calibrated so that the average SiteScore for 157 investigated submicromolar sites is 1.0; a score >1 suggests a site of particular promise for druggability. Application of SiteMap to the palmitoleate binding site of Notum (PDB: 4UZQ) generated a SiteScore of 1.2. Schrödinger Release 2019-3: SiteMap, Schrödinger, LLC, New York, NY, 2019. See, Halgren, T.A., Identifying and characterizing binding sites and assessing druggability. *J. Chem. Inf. Model.* **2009**, *49*, 377-389.

18.   Shoichet, B. K. Virtual screening of chemical libraries. *Nature* **2004**, *432*, 862–865.

19.   Willems, H.; De Cesco, S.; Svensson, F. Computational chemistry on a budget: supporting drug discovery with limited resources. *J. Med. Chem.* **2020**, *63*, 10158–10169.

20.   ChemDiv library, see: https://www.chemdiv.com/screening-libraries11/ (accessed Feb 10, 2021). The 952 compounds selected for screening in the biochemical Notum assay were purchased on Sep 17, 2019.

21.   Friesner, R. A.; Banks, J. L.; Murphy, R. B.; Halgren, T. A.; Klicic, J. J.; Mainz, D. T.; Repasky, M. P.; Knoll, E. H.; Shelly, M.; Perry, J. K.; Shaw, D. E.; Francis, P.; Shenkin, P. S. Glide: a new approach for rapid, accurate docking and scoring. 1. Method and assessment of docking accuracy. *J. Med. Chem.* **2004**, *47*, 1739–1749.

22.   Halgren, T. A.; Murphy, R. B.; Friesner, R. A.; Beard, H. S.; Frye, L. L.; Pollard, W. T.; Banks, J. L. Glide: a new approach for rapid, accurate docking and scoring. 2. Enrichment factors in database screening. *J. Med. Chem.* **2004**, *47*, 1750–1759.

23.   (a) Baell, J. B.; Holloway, G. A. New substructure filters for removal of pan assay interference compounds (PAINS) from screening libraries and for their exclusion in bioassays. *J. Med. Chem.* **2010**, *53*, 2719– 2740; (b) Baell, J. B.; Nissink, J. W. M. Seven year itch: pan-assay interference compounds (PAINS) in 2017 – utility and limitations. *ACS Chem. Biol.* **2018**, *13*, 36-44.

24.   (a) Blagg, J. Structure-activity relationships for *in vitro* and *in vivo* toxicity. *Ann. Rep. Med. Chem.* **2006**, *41*, 353-368; (b) Blagg, J. Structural Alerts for Toxicity. In *Burger's Medicinal Chemistry, Drug Discovery, and Development*, 7th ed.; Abraham, D. J., Rotella, D. P. Eds.; John Wiley & Sons: New York, 2010; pp 301-334; (c) Kalgutkar, A. S. Designing around structural alerts in drug discovery. *J. Med. Chem.* **2020**, *62*, 6276-6302.

25.   (a) Potashman, M. H.; Duggan, M. E. Covalent modifiers: an orthogonal approach to drug design. *J. Med. Chem.* **2009,** *52,* 1231-1246; (b) Singh, J.; Petter, R. C.; Baillie, T. A.; Whitty, A. The resurgence of covalent drugs. *Nat. Rev. Drug. Disc.* **2011**, *10*, 307-317.

26.   Ferreira, R. S.; Simeonov, A.; Jadhav, A.; Eidam, O.; Mott, B. T.; Keiser, M. J.; McKerrow, J. H.; Maloney, D. J.; Irwin, J. J.; Shoichet, B. K. Complementarity between a docking and a high-throughput screen in discovering new cruzain inhibitors. *J. Med. Chem.* **2010**, *53*, 4891–4905.

27.   Haneen, D. S. A.; Abou-Elmagd, W. S. I.; Youssef, A. S. A. 5(4*H*)-Oxazolones: Synthesis and biological activities. *Synth. Commun.* **2021**, *51*, 215-233.

28.   Blanco-Lomas, M.; Campos, P. J.; Sampedro, D. Benzylidene-oxazolones as molecular photoswitches. *Org. Lett.* **2012**, *1*, 4334-4337.

29.   Youssef, A. S. A.; Kandeel, K. A.; Abou-Elmagd, W. S. I.; Haneen, D. S. A. Action of some nitrogen and carbon nucleophiles on 4-arylidene-1,3-oxazolones. *J. Heterocycl. Chem.* **2016**, *53*, 175–182.

30.   For representative examples, see: (a) Yadav, L. D. S.; Sharma, S. A new route for the convenient synthesis of 5-acylamino-3,6-diarylperhydro-2-thioxo-1,3-thiazin-4-ones. *SYNTHESIS* **1992**, 919-920; (b) Yadav, L. D. S.; Singh, A. Microwave activated solvent-free cascade reactions yielding highly functionalised 1,3-thiazines. *Tetrahedron Lett.* **2003**, *44*, 5637-5640; (c) Habib, O. M. O.; Hassan, H. M.; Moawad, E. B.; El-Mekabaty, A. Reactivity of oxazolone derivative towards nitrogen and carbon nucleophilic reagents: applications to the synthesis of new heterocycles. *Int. J. Mod. Org. Chem.* **2013**, *2*, 11-25.

31.   Zhao, Y.; Svensson, F; Steadman, D.; Frew, S.; Monaghan, A.; Bictash, M.; Moreira, T.; Chalk, R.; Lu, W.; Fish, P. V.; Jones, E. Y. Structural insight of Notum covalent inhibition. *J. Med. Chem.* **2021**, *64*, 11354-11363. https://doi.org/10.1021/acs.jmedchem.1c00701

32.   Wager, T.T., Hou, X., Verhoest, P.R., Villalobos, A. Moving beyond rules: the development of a central nervous system multiparameter optimization (CNS MPO) approach to enable alignment of druglike properties. *ACS Chem. Neurosci.* **2010,** *1*, 435-449.

33.   Gupta, M.; Lee, H. J.; Barden, C. J.; Weaver, D. F. The Blood-brain barrier (BBB) score. *J. Med. Chem.* **2019**, *62*, 9824–9836.

34.   Jaguar DFT calculations for **4d** in the amide and iminol forms strongly favor the amide by about 13 kcal/mol (amide: -1155.9522 Ha; iminol: -1155.9314 Ha). This would suggest that ionization rather than tautomerization is the key driver for activity, along with steric fit for the methylated analogues. The measured pK_a of **4d** combined with the N2-H is likely to be significantly more acidic in the local environment of the binding pocket, due to stabilization by the oxyanion hole, supports this model. Calculations were performed using Jaguar version 10.5, release 13 at B3LYP-D3/LACV3P**+ level of theory with a PBF solvation model with default settings for water.

35.   (a) Manallack, D. T. The pK_a distribution of drugs: application to drug discovery. *Persp. Med. Chem.* **2007**, *1*, 25-38; (b) Manallack, D. T. The acid-base profile of a contemporary set of drugs: implications for drug discovery. *SAR QSAR Environ. Res.* **2009**, *20*, 611-655; (c) Manallack, D. T., Prankerd, R. J., Yuriev, E., Opera, T. I., Chalmers, D. K. The significance of acid/base properties in drug discovery. *Chem Soc. Rev.* **2013**, *42*, 485-496.

36.   For an excellent series of mini-perspectives describing drug metabolism and pharmacokinetic concepts as applied to drug design, see: (a) Smith, D. A.; Beaumont, K.; Maurer, T. S.; Di, L. Volume of distribution in drug design. *J. Med. Chem.* **2015**, *58*, 5691-5698; (b) Smith, D. A.; Beaumont, K.; Maurer, T. S.; Di, L. Clearance in drug design. *J. Med. Chem.* **2019**, *62*, 2245-2255; (c) Maurer, T. S.; Smith, D. A.; Beaumont, K.; Di, L. Dose predictions for drug design. *J. Med. Chem.* **2020**, *63*, 6423-6435.

37.   Qosa, H., Miller, D.S., Pasinelli, P., Trotti, D. Regulation of ABC efflux transporters at blood-brain barrier in health and neurological disorders. *Brain Res.* **2015**, *1628*, 298-316.

38.   Brommage, R.; Liu, J.; Vogel, P.; Mseeh, F.; Thompson, A. Y.; Potter, D. G.; Shadoan, M. K.; Hansen, G. M.; Jeter-Jones, S.; Cui, J.; Bright, D.; Bardenhagen, J. P.; Doree, D. D.; Movérare-Skrtic, S.; Nilsson, K. H.; Henning, P.; Lerner, U. H.; Ohlsson, C.; Sands, A. T.; Tarver, J. E.; Powell, D. R.;
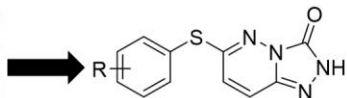
Zambrowicz, B.; Liu, Q. NOTUM inhibition increases endocortical bone formation and bone strength. *Bone. Res*. **2019**, *7*, 2.

39. Flanagan, D. J.; Pentinmikko, N.; Luopajärvi, K.; Willis, N. J.; Gilroy, K.; Raven, A. P.; Mcgarry, L.; Englund, J. I.; Webb, A. T.; Scharaw, S.; Nasreddin, N.; Hodder, M. C.; Ridgway, R. A.; Minnee, E.; Sphyris, N.; Gilchrist, E.; Najumudeen, A. K.; Romagnolo, B.; Perret, C.; Williams, A. C.; Clevers, H.; Nummela, P.; Lähde, M.; Alitalo, K.; Hietakangas, V.; Hedley, A.; Clark, W.; Nixon, C.; Kirschner, K.; Jones, E. Y.; Ristimäki, A.; Leedham, S. J.; Fish, P. V.; Vincent, J.-P.; Katajisto, P.; Sansom, O. J. NOTUM from *Apc*-mutant cells biases clonal competition to initiate cancer. *Nature* **2021**, *594*, 430-435.

40. Bender, B. J.; Gahbauer, S.; Luttens, A.; Lyu, J.; Webb, C. M.; Stein, R. M.; Fink, E. A.; Balius, T. E.; Carlsson, J.; Irwin, J. J.; Shoichet, B. K. A practical guide to large-scale docking. *Nat. Protoc.,* **2021**, *16*, 4799–4832.

41. Calculator Plugins were used for structure property prediction and calculation, Marvin 20.15, 2018, ChemAxon. http://www.chemaxon.com (accessed Mar 4, 2021).

42. Hill, A. P.; Young, R. J. Getting physical in drug discovery: a contemporary perspective on solubility and hydrophobicity. *Drug Discov. Today* **2010**, *15*, 648–655.

43. Brenk, R.; Schipani, A.; James, D.; Krasowski, A.; Gilbert, I. H.; Frearson, J.; Wyatt, P. G. Lessons learnt from assembling screening libraries for drug discovery for neglected diseases. *ChemMedChem* **2008**, *3*, 435–444.

44. Rankovic, Z. CNS physicochemical property space shaped by a diverse set of molecules with experimentally determined exposure in the mouse brain. *J. Med. Chem.* **2017**, *60*, 5943-5954. This mini-perspective was retracted on 2/5/2019 (*J. Med. Chem.* **2018**, DOI: 10.1021/acs.jmedchem.8b01388).

ToC Graphic
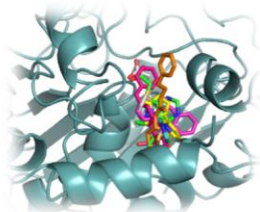
Docking-based Virtual Screen → New Series of Notum Inhibitors

4: IC$_{50}$ ≤ 10 nM